

MASTER'S THESIS

Course code: BIO5010

Name: Haakon Brandt Fjeld

Exploring density-habitat relationships and model
transferability for an alpine bird using abundance models

Date: 01.06.2021

Total number of pages: 47

Preface

This thesis is the final step on the road to graduating with a master's degree in biosciences with a specialization in terrestrial ecology and nature management. The education was conducted at campus Steinkjer, under the Faculty of Bioscience and Aquaculture at Nord University. Through the project *Willow ptarmigan ecology in a changing climate* (<https://lirypa.net/>), a project led by the Norwegian Institute for Nature Research (NINA) and Nord University, I have been privileged to be able to conduct research and a lot of fieldwork on my all-time favorite bird, the willow ptarmigan. I wish to thank my supervisor Erlend Birkeland Nilsen (Senior research scientist at NINA and Professor II at Nord University) for all the great discussions and for introducing me to the world of hierarchical distance sampling. And a big thank you to my supervisor Jan Eivind Østens (Associate professor at Nord University) for all the good feedback and for helping me through the writing process. I would also like to say a thank you to all the volunteer field personnel who have contributed with distance sampling surveys. Last but not least, I want to thank my fellow partners in crime (*Bubo baro*, *snowbed stine* and *Neovison martin*) who have inhabited the habitat patch known as the master room together with me for the last two years. Sadly, a highly invasive species (*student debt*) has reached us, so we must now disperse to new foraging grounds!

Håkon Brandt Fjeld

Nord University

June 2021

Abstract

Spatial predicting of species distribution and density using statistical models have become important in ecological studies. However, considerable challenges still exist for such models, partly caused by the complexity inherent in the species-habitat relationship. This can be addressed by modeling density and detectability as a function of habitat within a hierarchical distance sampling framework (HDSM). However, due to a range of biotic and abiotic factors, variations in the relationship between density and habitat can vary in time and space. As a consequence, models developed on data from a particular time and place might not predict accurately or precisely in novel conditions, an issue referred to as model transferability.

The first step in this thesis was to explore the relationship between willow ptarmigan (*Lagopus lagopus*) density and habitat characteristics through the use of HDSM. Secondly, model transferability was assessed in time (across years) and space (across six study areas in central Norway). To assess transferability, I established models with environmental covariates from two different spatial scales (home range and landscape scale, respectively). At both scales, I estimated the habitat-density relationships in six different areas using appropriate data from the years 2016-2020 (a total of 2 x 22 models). Transferability was assessed by comparing predicted densities (estimated with non-local data) to observed densities (estimated with local data) in 500 x 500m grid cells using Pearson's correlation. Finally, linear regressions were used to explore how different variables affected model transferability. In particular, I assessed how spatial and temporal distance between or within areas affected transferability.

Considerable variations in the estimated habitat-density relationship and model transferability were identified at both spatial scales. Regression analyses revealed that models from both scales transferred best between years in the same area compared to transferability among areas. Furthermore, there were some support for decreased spatial transferability, as distance between areas increased. Regarding spatial scale, models established with landscape covariates transferred better to other areas, compared to models established with home range scaled covariates. However, the transferability in the same area between years was less affected by spatial scale. This thesis demonstrates the benefit of using localized data and calls attention to the problem of predicting density/abundance in novel areas, particularly for a bird species with a short life span and large inter-annual fluctuations in abundance, such as the willow ptarmigan.

Keywords: Hierarchical distance sampling, transferability, alpine bird, *Lagopus lagopus*, tetraonidae, habitat specific density, abundance models.

Sammendrag

Predikeringer av arters habitatbruk ved hjelp av statistiske modeller har blitt svært vanlig i økologiske studier. Som følge av kompleksiteten i arters habitatbruk er det imidlertid betydelige utfordringer knyttet til disse modellene. Dette kan delvis løses med bruk av hierarkiske avstandsmodeller (HDSM), hvor tetthet og oppdagbarhet blir modellert som en funksjon av habitat. Likevel kan økologisk dynamikk skape variasjon i forholdet mellom tetthet og habitat. Dette betyr at modeller utviklet med lokal data fra et gitt sted, og et gitt år, ikke nødvendigvis predikerer tettheten presist og nøyaktig i andre områder eller under nye forhold. Dette kan bli evaluert med et kvantitativt mål, også kjent som modelloverførbarhet.

Det første steget i denne oppgaven var å undersøke sammenhenger mellom habitat og tettheter av lirype (*Lagopus lagopus*) ved bruk av HDSM. I neste steg ble modelloverførbarhet undersøkt i tid (mellom år) og rom (mellom seks områder i Midt-Norge). Dette ble gjennomført ved bruk av to modeller etablert med kovariater fra to ulike rommelige skalaer (leveområde- og landskap modell). Basert på de to modellene ble forholdet mellom habitat og tetthet estimert i seks ulike områder ved å benytte egnede takseringsdata fra årene 2016-2020 (Totalt 2 x 22 modeller). Modelloverførbarhet ble deretter målt med korrelasjon mellom observerte tettheter (estimert med bruk av lokal-data) og predikerte tettheter (estimert med ikke-lokal data) i 500 x 500m ruter som dekket de seks ulike områdene. Til slutt ble regresjonsanalyser brukt for å undersøke hvordan ulike variabler påvirket modelloverførbarheten. I den forbindelse ble avstand mellom områder, rommeligskala og overførbarhetstype (tid eller rom) brukt som forklaringsvariabler.

Betydelige variasjoner ble identifisert både for modelloverførbarheten og i habitat-tetthet forholdet for begge rommelige skalaer. Dette betyr at forholdet mellom habitat og rypetetthet i rutene kan være ulike både mellom områder og år. Regresjonsanalysen viste at modeller fra begge rommelige skalaer var lite overførbare mellom ulike områder, sammenlignet med overførbarhet innad i samme områder imellom år. Et hovedfunn var at overførbarheten ble redusert når avstand mellom områdene økte. I henhold til rommelig skala, var modeller etablert med kovariater fra landskapsskala mer overførbare mellom områder enn modeller etablert med kovariater fra leveområdeskala. Denne forskjellen var mindre klar for intern overførbarhet i samme område mellom år. Resultatene i denne oppgaven viser fordelene med bruk av lokale data og påpeker samtidig utfordringer med å predikere tettheter til andre områder uten noe form for innsamlede data, spesielt for en alpin art med store populasjonsfluktuasjoner slik som lirype.

Contents

1.0 Introduction	1
2.0 Material and methods	5
2.1 Study areas	5
2.2 Field data.....	6
2.3 Data preparations	6
2.4 Environmental covariates.....	7
2.4.1 Landcover data.....	8
2.4.2 Topography	8
2.4.3 NDVI.....	9
2.4.4 Human disturbance	9
2.5 Statistical analyses and model selection	9
3.0 Results	12
3.1 Home range models	12
3.2 Landscape models.....	12
3.3 Variation in covariate-effects across time and space (home range scale).....	13
3.4 Variation in covariate-effects across time and space (landscape scale).....	15
3.5 Transferability	16
3.6 Factors affecting transferability	18
4.0 Discussion	20
4.1 Variations in covariate effects.....	20
4.2 Variations in model transferability	23
5.0 Management implications and concluding remarks.....	24
Literature	25

Appendices

Appendix A	1
Appendix B	2
Appendix C	3
Appendix D	4
Appendix E.....	5
Appendix F.....	6
Appendix G	7
Appendix H	8
Appendix I.....	9
Appendix J.....	10
Appendix K	11
Appendix L.....	12

1.0 Introduction

Ecology can be defined as “*the scientific study of the interactions that determine the distribution and abundance of organisms*” (Kerbs, 1972). Consequently, estimates of abundance are fundamental properties in ecology (Buckland *et al.*, 2001). This has led to considerable research investment in order to develop models to sample and estimate abundances of species under various conditions (e.g. Seber, 1986; Schwarz & Seber, 1999; Wilson & Delahay, 2001). An approach that can be applied to particular species in certain habitats is total counts (Talbot & Stewart, 1964; Orpin *et al.*, 1985) however, this is in general time-consuming, expensive, and often unreliable because of observation errors (Fryxell *et al.*, 2014). Thus, alternative methods that specifically model observation or detection probability is generally advocated (Buckland *et al.*, 2015). Some of these methods are based on the physical marking of individuals (Borchers *et al.*, 2002; Williams *et al.*, 2002), however, in many cases such methods are not attainable due to e.g., logistical constraints, creating a demand for methods that do not rely on marked individuals but that are still robust to observation uncertainty. One such approach is the distance sampling (DS) method (Buckland *et al.*, 2001), which is one of the most widespread frameworks for estimating the abundance and/or density of unmarked wildlife populations (Williams *et al.*, 2002; Royle *et al.*, 2004; Sillett *et al.*, 2012). The basic principle of DS is to describe the detection probability with the use of distances from a point or line to an observed individual. Thereafter the relationship between distance and the number of observed individuals is used to estimate density (number of individuals/pr unite area) or abundance (total number of individuals in an area) (Buckland *et al.*, 2001).

The abundance or density of a wild species is not homogenous in time and space (Buckland *et al.*, 2001; Guisan *et al.*, 2017). It is rather shaped by the environment through a complex and dynamic interplay with biotic factors such as competition and predation, or abiotic variables such as climate, soil, and bedrock (Woodward & Williams, 1987; Chamberlain & Fuller, 1999; Wisz *et al.*, 2013; Guisan *et al.*, 2017). To illustrate this, Sillett *et al.* (2012) provided an example of how the distribution and density of the island scrub-jay (*Aphelocoma insularis*) increased as a response to the removal of domesticated herbivores and the recovery of native vegetation. In addition, human impacts often play a major role in shaping distributions and density since disturbance effects or habitat fragmentation can reduce the access to areas that otherwise would have been exploited (Lens *et al.*, 2002; Gill, 2007; Brøseth & Pedersen, 2010; Fryxell *et al.*, 2014). The interaction between species and their environments creates a challenge

for the traditional DS and other statistical methods used to estimate the size of a population (Royle *et al.*, 2004; Chandler *et al.*, 2011; Sillett *et al.*, 2012). One method that acknowledges the relationship between the density of a species and its environment, and simultaneously accounts for variation in detection probability, is an extension of the traditional DS termed hierarchical distance sampling models (hereafter HDSM) (Royle *et al.*, 2004). A practical application of HDSM is the possibility to produce spatial predictions of species density within grid cells in a focal area as a function of environmental covariates (land cover, vegetation height, vegetation composition, etc.) (Sillett *et al.*, 2012; Roach *et al.*, 2017; Furnas *et al.*, 2019).

Predictive modeling is a process that seeks to predict the unknown, for instance the state of a system (ecological or otherwise) in an area or time of interest and beyond the area for which utilized for model fitting (Mouquet *et al.*, 2015; Yates *et al.*, 2018). Predictive models can provide valuable knowledge for decision-making through mapping of species density, distribution, population trends, or the risk of biological invasions (e.g., Sillett *et al.*, 2012; Mouquet *et al.*, 2015; Urban *et al.*, 2016). However, the complexity in ecological processes implies that predictive models developed with local data from a particular time and place (training data), might not predict accurately or precisely into novel conditions. This issue is often referred to as model transferability (Sequeira *et al.*, 2018; Yates *et al.*, 2018). Several factors have been highlighted as possible reasons for poor transferability, including species traits, sampling biases, biological interactions, non-stationarity, and the degree of environmental dissimilarity between reference and target areas (e.g., habitat availability) (Yates *et al.*, 2018).

In order to develop a spatial model of species distributions or habitat-density relationships with high predictive power, and effective spatial and temporal transferability, covariates need to have ecological relevance while avoiding location-specific relationships that are not consistent across time and space (Guisan & Thuiller, 2005). This is a difficult task as there might be a lack of knowledge of relevant predictor covariates, and yearly and site-specific variation in ecological processes is common (Guisan & Zimmermann, 2000; Yates *et al.*, 2018; Avgar *et al.*, 2020). For instance, some species experience variance in the degree of top-down control from predation (Breisjøberget *et al.*, 2018). Variation in habitat availability can also compromise the utility of a predictive model, because species can change preference for a given

type of habitat as a response to habitat availability (known as a functional response in habitat use; (Myserud & Ims, 1998)). Variations in habitat use can also be explained by density dependence (Avgar *et al.*, 2020). This is often illustrated with the theoretical concept known as ideal free distribution (Fretwell, 1969), where species select habitats with different suitability as a response to their density. This implies that the transferability of predictive abundance models might be questionable for species with a high variance in demography. As an example, Gray *et al.* (2009) reported that differences in breeding density of a tropical bird, the bengal florican (*Houbaropsis bengalensis*), most likely affected the transferability of a species distribution model.

When assessing and including covariates, the spatial scale must be considered both in relation to grain (sampling resolution) and/or extent (range of study area) (Turner *et al.*, 2001). This is important because habitat selection can occur on several spatial scales (Johnson, 1980; Mayor *et al.*, 2009). Often the researcher knows where a species normally occurs on a landscape scale, known as the “*the no elephants in the artic effect*” (Lobo *et al.*, 2010; Loe *et al.*, 2012). In contrast, there is often more uncertainty related to how species are distributed on a finer spatial scale (Loe *et al.*, 2012). For example, on a home range scale, individuals must select for different habitat components within a landscape that fulfill demands in relation to food, shelter, breeding sites, and so on (Burt, 1943). For this reason, there is often a trade-off between good model transferability and accuracy (Gottschalk *et al.*, 2011; Loe *et al.*, 2012; Manzoor *et al.*, 2018). An example of such a trade-off can be found in Loe *et al.* (2012), who shows how a species distribution model of red deer (*Cervus elaphus*) performed best on a landscape scale compared to a home range scale, explained by a trivial and already recognized effect of avoidance of barren mountain habitats.

Assessment of transferability is complex, but nonetheless important since the transfer of an inaccurate predictive model to areas with no sampling data might lead to biased population estimates, poor habitat assessments (Roach *et al.*, 2017), and unsustainable management decisions (Muscatello *et al.*, 2020). In this thesis, HDSM with environmental covariates is developed for willow ptarmigan (*Lagopus lagopus*) populations in different areas of central Norway, in order to assess the transferability of habitat-abundance models in time and space. The willow ptarmigan is a medium-sized bird, with a short lifespan, inhabiting alpine ecosystems, often with high-multi annual cycles in population density (Myrberget, 1988; Steen

& Erikstad, 1996). Previous knowledge suggests that willow ptarmigans prefer open habitats with shrubs and that they usually avoid denser forests at lower altitudes and barren habitats at higher altitudes (Hannon *et al.*, 1998; Potapov & Sale, 2013). On a home range scale, vegetation consisting of willow species (*Salix spp.*) and dwarf birch (*Betula nana*) are described as important components affecting the presence of willow ptarmigan (Andersen *et al.*, 1984; Steen *et al.*, 1985; Kastdalen *et al.*, 2003; Henden *et al.*, 2011; Ehrich *et al.*, 2012). There is also evidence that the willow ptarmigan avoids lichen-rich heathlands and usually selects herb-dominated areas and bogs (Andersen *et al.*, 1984; Kvasnes *et al.*, 2017; Kvasnes *et al.*, 2018). Additionally, ptarmigan habitat-use can in certain cases be affected by disturbance effects (Brøseth & Pedersen, 2010). Based on this knowledge, environmental covariates from different spatial scales were included in the HDSM's. and models were used to explore habitat-density relationships and possible transferability issues. This was approached through three objectives:

- The first objective was to estimate habitat-density relationships in six areas with data spanning from 2016-2020 with the use of a model with home range scaled covariates and a model with landscape scaled covariates (in total 2x22 models). Based on these models, the consistency of the habitat-density relationship was assessed.
- The second objective was to assess model transferability among years and areas. Transferability was assessed by comparing predicted density calculated with out of sample predictions (to novel areas or between areas) with observed densities calculated with the focal models (2x22 models).
- The last objective was to explore factors that could contribute to variation in model transferability. In particular, I assessed how distance between areas, spatial scale, and type(spatial/temporal) of transferability affected the measured model transferability.

2.0 Material and methods

2.1 Study areas

Six sampling areas were selected from a grouse species (*tetraonidae spp.*) monitoring program covering a large proportion of alpine areas in Norway, called Hønsefuglportalen (<https://honsefugl.nina.no/>). The areas included in the study were selected on the basis of east-west and north-south gradients across central parts of Norway (Figure 1). The intention of this study design was to assess model transferability within this region by simultaneously including areas with both variation and similarities in climate, vegetation, and the amount of infrastructure (Appendix A1 and A2). Central Norway was used as the focal region in this study because it is an important region for recreational hunters in Norway (Pedersen & Storaas, 2013). Consequently, an evaluation of the application of an HDSM might be valuable for the local management. Additionally, the selection of areas was assumed to be sufficient to explore and present possible results concerning variation in habitat-density relationships, and model transferability that is also relevant for other regions.

Areas 1, 3, 5, and 6, are located in continental areas with low humidity and cold winters, area 2 is located at the coast with high humidity and warmer winters, while area 4 is located in a transitional zone with a relatively humid climate and warm winters (Moen *et al.*, 1998). This variation in climate forms the foundation for the heterogeneous landscape in the

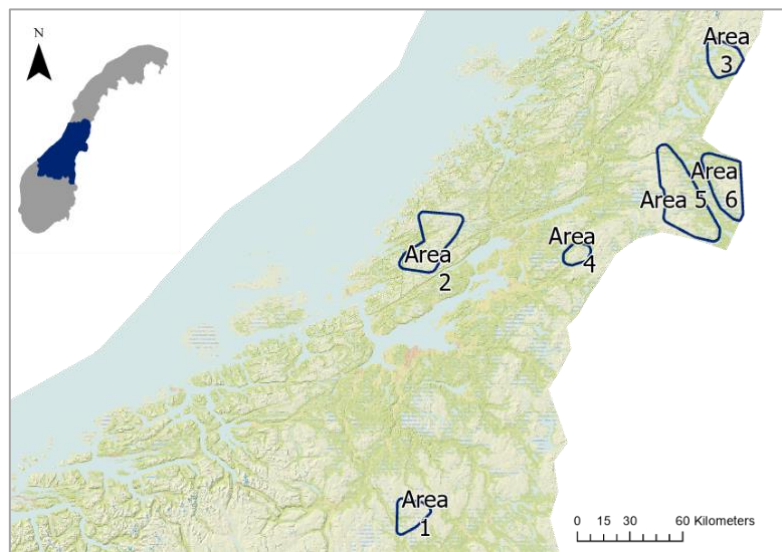


Figure 1: The location of central Norway (top left) and the six study areas (1 = Forollhogna, 2 = Aaffjorden, 3 = Rooyrvik, 4 = Steinkjer, 5 = Lierne west, 6 = Lierne east).

region. Which is characterized by valleys, boreal forests, agricultural areas, bogs/swamps, developed areas, and mountains. All six study areas have alpine habitats at higher altitudes, typically with moderately steep and rugged terrain, with a landscape consisting of a mosaic of bogs, forests, and alpine vegetation dominated by dwarf birch (*Betula nana*), *Salix spp.* and *Ericaceous spp.* Around the tree line the vegetation consists mostly of birch (*Betula spp.*) and/or a mosaic of pine (*Pinus sylvestris*) and spruce (*Picea abies*).

2.2 Field data

Sampling data used to fit HDSM's were collected through the monitoring program Hønsfuglportalen, which is based on line-transect surveys and DS (Buckland *et al.*, 2001; Kvasnes *et al.*, 2019). The transects were surveyed annually in August, by a team of two or more volunteers. Not all or the same transects were surveyed every year because of practical reasons. The field personnel followed pre-defined transects using a field protocol. In most cases, the transects were distributed systematically following a map grid with 500m intervals, and often in north-south or east-west direction (Appendix B1). Free-running, trained dogs was used to search for birds on both sides of the transect (Pedersen *et al.*, 2004; Warren & Baines, 2011; Kvasnes *et al.*, 2015). Both single ptarmigan individuals and clutches with several birds were reported as an observation (Buckland *et al.*, 2001). For each of those observations the number of birds in the clutch, GPS coordinates, and the perpendicular distances from the transect line to the observation were recorded. In addition, the length, and position of the transect were recorded. Data from monitoring programs for *tetraonidae spp.* across Norway are available through www.gbif.com (Nilsen *et al.*, 2020 a; Nilsen *et al.*, 2020 b).

2.3 Data preparations

Data from surveys with equal study design (no curved or angled line-transects) from the period of 2016-2020 were used in the analyses. All transects ($n = 207$) were divided into 500m long segments ($n = 1223$). Some of the lines had lengths that did not match the interval, hence the last segment at the end of these lines was less than 500m, these end segments were removed, so that all segments had an equal size. A buffer of 250m was added on each side of the segment, resulting in 500 x 500m segments (Appendix B2). These were all given a unique id. This process was done to be able to include environmental covariates at the desired level (Miller *et al.*, 2013) and to simplify spatial predictions for the entire study area. The observations of ptarmigans were linked to the segments using the segment id and year (Table 1), and only observations of ptarmigans recorded within the 250m buffer were kept for further analyses ($n = 2565$). Finally, the perpendicular distances from observations to the line was pulled into 25 meters intervals, making it possible to use the data in the *distsamp* function in the R package; *unmarked* (Royle *et al.*, 2004; Fiske & Chandler, 2011; Sillett *et al.*, 2012; Le Moullec *et al.*, 2017). The choice of segment size was based on several ideas, first, the segments needed to be large enough to contain several observations with different perpendicular distances to the transect line. In addition, it was beneficial to have enough segments per line, to increase the

ability to detect the effects of habitat heterogeneity (Le Moullec *et al.*, 2017). Furthermore, Miller *et al.* (2013) proposed segments to be sized in a way that neither density of objects, nor covariate values are significantly different from each other. Miller *et al.* (2013), also states that making segments $2w \times w^2$, where w is the truncation distance should be sufficient. The use of 500 x 500m segments in this thesis was an attempt to meet some of these elements. However, I did not assess further how the habitat-density relationships presented in this thesis are affected by the segment size. It is therefore advisable to approach the habitat-density relationship presented in this thesis with some caution.

Table 1: The total number of 500 x 500m segments used to establish hierarchical distance sampling models. In addition, the total number of observations (ptarmigan clutches or single individuals) and segments with at least one observation is included. Surveys with a different study design were left out and are marked n/a.

Survey years	Area 1	Area 2	Area 3	Area 4	Area 5	Area 6
2016						
Number of segments:	206	n/a	n/a	n/a	n/a	n/a
Segments with at least one observation:	103	n/a	n/a	n/a	n/a	n/a
Total number of observations:	146	n/a	n/a	n/a	n/a	n/a
2017						
Number of segments:	206	n/a	n/a	76	297	177
Segments with at least one observation:	110	n/a	n/a	28	81	46
Total number of observations:	190	n/a	n/a	33	106	64
2018						
Number of segments:	206	n/a	92	74	296	177
Segments with at least one observation:	140	n/a	37	32	92	45
Total number of observations:	283	n/a	74	47	137	62
2019						
Number of segments:	206	232	117	76	296	174
Segments with at least one observation:	130	59	72	32	102	68
Total number of observations:	286	79	114	41	150	114
2020						
Number of segments:	197	236	106	76	272	168
Segments with at least one observation:	110	59	43	30	99	55
Total number of observations:	212	82	81	46	138	80

2.4 Environmental covariates

To process categorical and numerical covariates used to establish HDSM's, ArcGIS pro version 2.6.0 was used. All the covariates used in the study were derived from raster datasets with the same cell size (30 x 30m) and the same spatial reference (WGS 1984 / UTM sone 33).

2.4.1 Landcover data

The percentage coverage of different vegetation types in each segment was extracted from a 30 x 30m digital-raster map that covers all of Norway (satVeg). SatVeg is a freely available land cover map derived from satellite images and ground surveys and is available for download through the Norwegian environmental agency: <https://kartkatalog.miljodirektoratet.no/>. The satellite imagery (Scenes from 1988-2006) used in satVeg are obtained from Landsat 5/TM and Landsat 7/ETM+ (Johansen B. E, 2009; Johansen *et al.*, 2009). The original classification consisted of 25 different vegetation categories. To simplify the model selection procedure and in an attempt to use categories that are ecological meaningful, the 25 original categories were reclassified. Five of these categories were irrelevant for the study and were removed (Appendix C1). The remaining 21 categories were used to produce two different raster maps used in two different analyses. The two maps had different spatial scales in relation to sampling resolution, hereby referred to as landscape scale (LS) and home range scale (HR). In the LS map, the 21 SatVeg categories were grouped in forested areas (FA) and open areas (OA), similar to the classification done by Brøseth and Pedersen (2010). Secondly, the 21 SatVeg categories in the HR map were categorized into seven groups: mountain birch forests (MB), swamps and bogs with sparse field layer (BSF), bogs with dense field layer (BDF), open areas with sparse field layer (OSF), open areas with dense field layer (ODF), snowbed vegetation (SB) and lowland/boreal forests (LF), similar to the classification in Kvasnes *et al.* (2017).

2.4.2 Topography

For each 500 x 500m segment, the mean elevation (meters above sea level) was extracted from a 30 x 30m digital elevation model (DEM) using all the DEM cells within the segments (Figure 2). This data was downloaded from the Norwegian Mapping Authority (<https://kartkatalog.geonorge.no/>). The same DEM model was also used to create a digital-raster map of the slope. The mean slope value (in degrees) was then calculated and extracted for each unique segment using the same procedure as for the mean elevation.

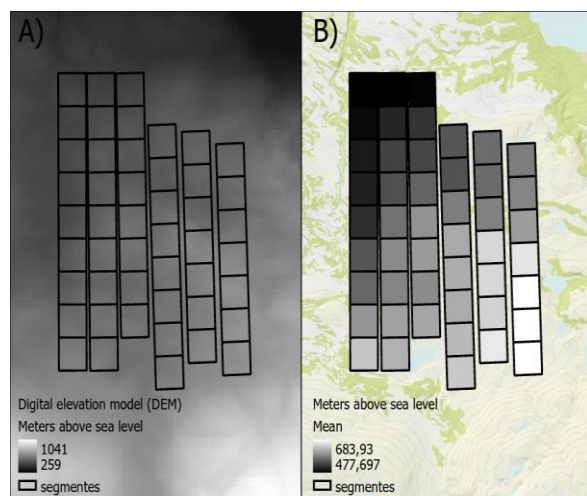


Figure 2: map A) 30 x 30m digital elevation map (DEM) and 500 x 500 segments. Map B) The mean value in meters extracted from the DEM to the segments.

2.4.3 NDVI

Measures of vegetation greenness were included using the normalized difference vegetation index (NDVI). NDVI is a spectral index based on the ratio between regions of the electromagnetic spectrum: $NDVI = \frac{NIR - RED}{NIR + RED}$, where NIR and RED are the amounts of near-infrared and red light, reflected by vegetation and captured by sensors (Pettorelli *et al.*, 2005). The NDVI is presented with values ranging from -1 to 1, where negative values correspond to an absence of vegetation (Myneni *et al.*, 1995). Seven 10 x 10m satellite photos taken by Sentinel-2A were downloaded from <https://earthexplorer.usgs.gov/>. The cloud cover was less than 20 % for all images, and only august images were used to match the month when the distance sampling surveys were conducted. However, the year of the images differed from 2016 to 2020. The 10m resolution images were used because these had NIR and RED values. After calculating the NDVI, the raster was resampled to 30 x 30m, with a bilinear technique suitable for continuous data (Baboo & Devi, 2010). The 30 x 30m raster was then used to calculate the mean NDVI for each unique segment, using the same approach as done for the topography datasets (Chapter 2.4.1).

2.4.4 Human disturbance

Spatial data of roads and buildings were obtained from the N50 dataset, available for download at the Norwegian Mapping Authority; <https://kartkatalog.geonorge.no/>. The road data consist of lines with gravel roads, private roads, and public roads. For the building data, a selection was made so only recreational buildings (cabins, tourist cabins, etc.) were used further. For both sets of spatial data a multiple ring buffer with 200m intervals was added and thereafter processed to two independent 30 x 30m rasters. Finally, the mean distance (meters) from roads and cabins was calculated using the cell values from the two independent rasters, for each of the unique segments, using the same approach as done above (Chapter 2.4.1).

2.5 Statistical analyses and model selection

HDSM's were established with the *distsamp* function available in the R-package *unmarked* (Royle *et al.*, 2004; Fiske & Chandler, 2011), through the use of RStudio (R Core Team, 2021). Before building model candidates, a spearman's rank correlation was employed to test for multicollinearity among all the environmental covariates (Appendix D1 and D2). Covariates with a negative or positive correlation larger than 0,55 (spearman's rho) were not implemented

in the same sub-model. Different combinations of the covariates were then used to compute sub-models for detection (σ) and density (λ) simultaneously. To avoid over-parameterization, a maximum of 6 parameters (4 covariates, detection parameter, and density parameter) were included in each model, as proposed by Le Moullec *et al.* (2017). The half-normal detection function was used for all the models, with the assumption that the detection probability decreases monotonically as the distance from the transects increases (Buckland *et al.*, 2001) (Appendix E1).

To identify important covariates affecting density, survey data from a random reference area (area 5 in 2017) was used to fit model candidates. Two model selection procedures using the Akaike information criterion (AIC) (Akaike, 1974), was then conducted; one for home range model candidates ($n = 40$), and one for landscape model candidates ($n = 4$) (Appendix F1). Both linear and quadratic terms were used to model the covariate effect on the density parameter (λ). For the detection parameter (σ), I assumed that the proportion of open areas with dense field layer (ODF) were important in the home range models. For the landscape models, I assumed that the proportion of forested areas (FA) had the strongest effect on the detectability (Appendix G1 and G2). The models with the most support from the two model selection procedures were used further to assess model transferability in time and space.

Before assessing transferability a test of model accuracy was conducted for all the candidate models fitted on the reference area, using k-fold cross-validation with the *crossval* function available in the *unmarked* package (Fiske & Chandler, 2011). In this process 3-folds were used, meaning that the survey data was split into three groups (folds), where one of the folds was then used as a training set and the remaining three were kept for validation. This process was repeated so that all three folds were used as a training set. The mean absolute errors (MAE) between the training and validation sets were then used to rank the models. The MAE is more precisely the mean value of all the individual differences between the predictions in the training set and the observations in the validation set (residuals) (Mayer & Butler, 1993).

To assess transferability of the predictive HDSM's, correlation tests were performed between observed and predicted ptarmigan densities. The following approach was used:

- Raster maps for each study area with 500 x 500 m grid cells were prepared (study area raster's). The percentage of landcover and the mean values of numerical covariates were calculated for each of the cells in the study area raster's, following the same procedure as for the segments (chapter 2.4).
- Next, the *predict* function in the R-package; *unmarked* (Fiske & Chandler, 2011) was used to estimate the number of ptarmigans in each of the grid cells in the study area rasters. This was done by using survey data for the given study area for the given year (local data) in the models with the most support in the reference area (Herby referred to as observed density).
- Also, estimations of the number of ptarmigans in each of the grid cells in the study area rasters were estimated using predictive models established with external non-local data from the different years and study areas (herby referred to as the predicted density).
- To assess the overall spatial and temporal model transferability, Pearsons correlation tests were performed between all the combinations of observed and predicted densities between study areas (external transferability) or the same study area in different years (internal transferability) (See appendix H1 for an example).
- In the final step, distances in kilometers (km) between the center of the study areas were calculated. This was then implemented in multiple linear regressions using the *lm* function in the R-package: R-stats (R Core Team, 2021). The transferability (raster correlations) was used as the response variable while distances, spatial scale (home range or landscape), and the type of transferability (spatial/temporal) were used as explanatory variables.

3.0 Results

3.1 Home range models

At the home range scale, one of the models applied to the reference area (area 5 in 2017) was within $\Delta AIC < 2$ (Table 2, Appendix I1). This model (model 20) had two covariates affecting density (λ): open sparse field layer (ODF) and bogs with sparse field layer (BSF). Model accuracy from the 3-fold cross-validation were in general good. With only small variations in MAE-values and standard deviation (SD) between all candidate models fitted to data from the reference area, with MAE ranging from 0.19 to 0.34 (Appendix F1). The highest-ranking model was among the least accurate models, with a mean difference of 0.32 (SD \pm 0.003) ptarmigans/per grid cell between the training and validation set.

Table 2: Akaike information criterion (AIC) values for the null model, and the five highest-ranked home range model candidates. Covariates that affect the shape parameter for a half-normal detection function (σ) and density (λ) are presented.

Home range models	Covariates	Parameters (n)	AIC	ΔAIC	AICwt.	Cum. Wt.
Model 20:	ODF (σ) \sim OSF + BSF (λ)	5	3713.34	0.00	0.91	0.91
Model 16:	ODF (σ) \sim OSF + slope ² (λ)	6	3719.90	6.56	0.03	0.95
Model 19:	ODF (σ) \sim OSF + BDF (λ)	5	3720.76	7.42	0.02	0.97
Model 28:	ODF (σ) \sim OSF ² (λ)	5	3722.04	8.70	0.01	0.98
Model 4:	ODF (σ) \sim OSF (λ)	4	3722.10	8.76	0.01	0.99
Model 1:	(σ) \sim (λ)	2	3760.84	47.50	< 0.01	1.00

3.2 Landscape models

One landscape model applied to the reference area (area 5 in 2017), were within $\Delta AIC < 2$ (Model 44). The density parameter for this model (Table 3, Appendix I2) had a quadratic term for forested areas (FA), implying a non-linear relationship. In the case of model accuracy, the MAE was equal for the five landscape model candidates, with only a small difference in the standard deviation (Appendix F1) (model 44: MAE = 0.32, \pm 0.01).

Table 3: Akaike information criterion (AIC) values for the null model, and all the landscape model candidates. Covariates affecting the shape parameter for a half-normal detection function (σ) and density (λ) are presented.

Landscape models:	Covariates	Parameters	AIC	ΔAIC	AICwt.	Cum. Wt.
Model 44:	FA (σ) \sim FA ² (λ)	5	3734.08	0.00	1.00	1.00
Model 43:	FA (σ) \sim OA ² (λ)	5	3745.11	11.03	0.00	1.00
Model 41:	FA (σ) \sim OA (λ)	4	3753.33	19.25	0.00	1.00
Model 42:	FA (σ) \sim FA (λ)	4	3754.98	20.90	0.00	1.00
Model 1:	(σ) \sim (λ)	2	3760.84	26.76	0.00	1.00

3.3 Variation in covariate-effects across time and space (home range scale)

Based on the home range model with the strongest support from the procedure above, I next estimated covariate effects (for model 20) using sampling data from all six study areas. There was a substantial variation in covariate effects (Figure 3). The responses were for some areas more conclusive, e.g., a clear significant negative response was observed for area 1 in all years included. Significant negative responses in density were also observed in area 3. In contrast to this, positive responses were observed in areas 2, 4, 5, and 6. Nevertheless, some of the response curves only showed slight changes, as the percentage coverage of OSF changed, for instance in the years 2017 and 2019 in area 6.

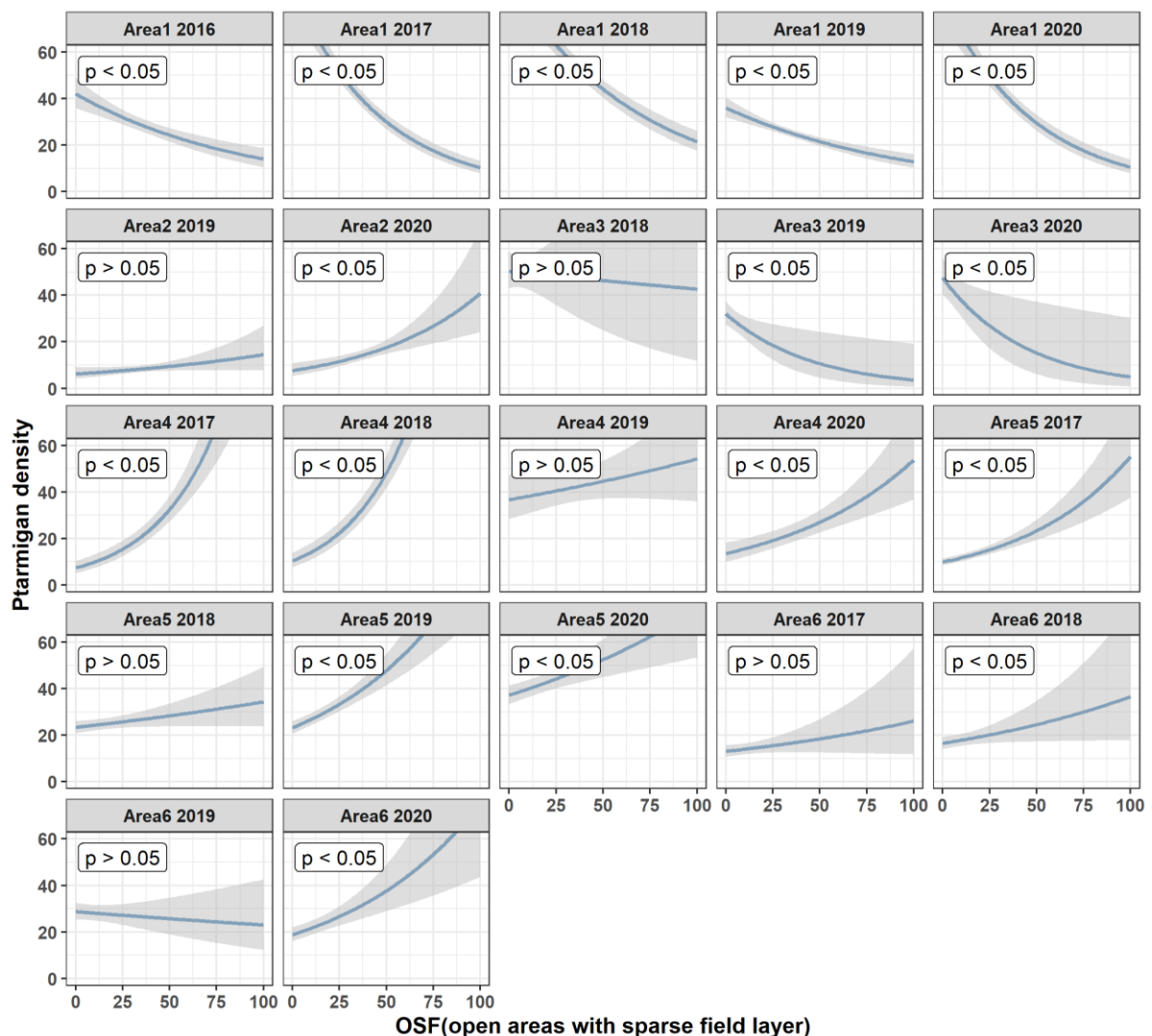


Figure 3: Willow ptarmigan density (birds/per 500x500m grid cell) as a function of the percentage coverage of open areas with sparse field layer (OSF) in six different study areas in different years. Estimated values (solid line) are plotted with a 95 % confidence interval (grey fill). The p-value for the OSF parameter estimate is included in the labels.

Similar to the covariate effect of OSF, the relationship between estimated ptarmigan density and the percentage coverage of bogs with sparse field layer (BSF) was heterogenous between areas and years (Figure 4). More precisely, in most areas and years, there were only small changes (positive and negative) in density as the coverage of BSF increased. In spite of this, some areas also had steep increases/decreases in density as a response to coverage change of BSF. For instance, area 1 in 2020 and area 4 in 2017.

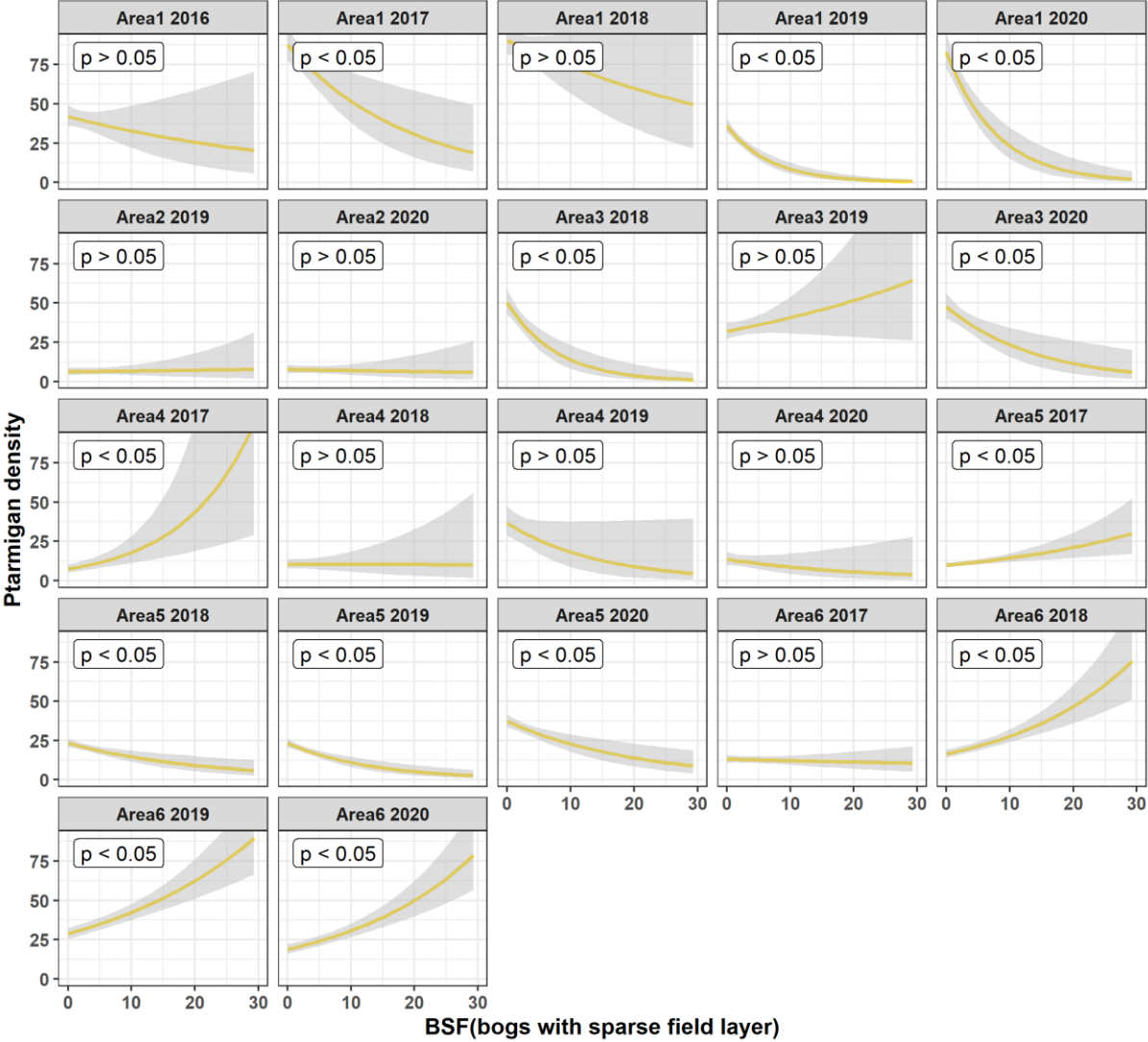


Figure 4: Density (ptarmigans/per 500x500 m grid cells) as a function of the percentage coverage of bogs with sparse field layer (BSF) in six different study areas in different years. Estimated values (solid line) are plotted with 95 % confidence intervals (grey fill). The p-value for the OSF parameter estimate is included in the labels.

3.4 Variation in covariate-effects across time and space (landscape scale)

Based on the landscape model with the strongest support (model 44) in the model selection procedure, I estimated covariate effects using model 44 and sampled data from all six study areas (Figure 5). The pattern in the response plots had some variation between the different study areas in the years included. In most cases, the estimated ptarmigan density was highest from around 30 to 60 % coverage of FA in the areas with an inverted u-shape relationship between FA and density. Nonetheless, there were also areas with no clear top in the density as a function of FA. On the contrary area 4 in 2019 had a u-shape relationship, with a lower peak of around 30 % coverage. The same pattern was also seen in area 5 in 2018 and 2020, but only with a small changes of density as the coverage increased.

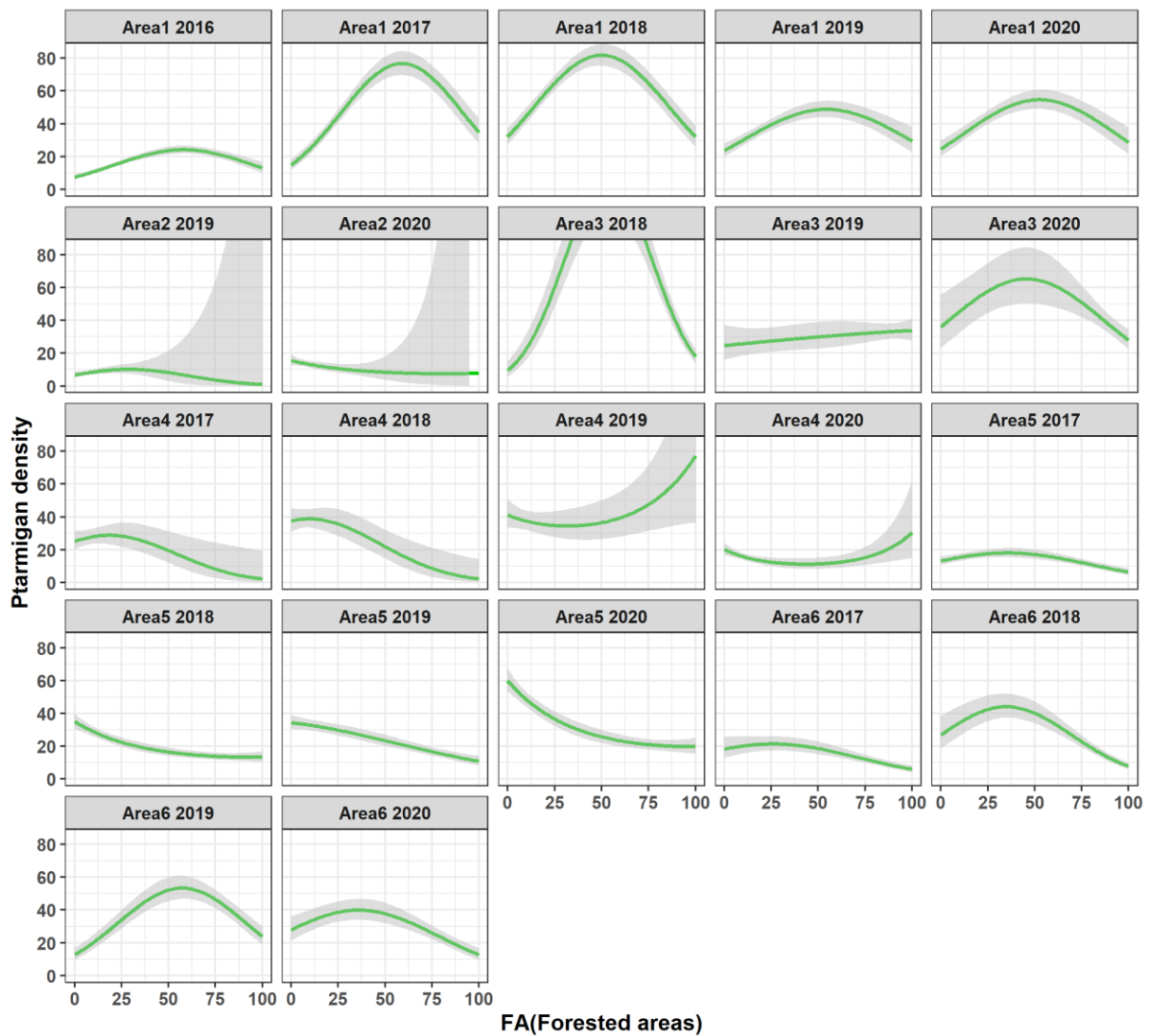


Figure 5: Density (ptarmigans/per 500x500 m grid cell) as a function of the percentage of forested areas (FA), in the six different study areas in different years. Estimated values (solid line) are plotted with 95 % confidence intervals (grey fill).

3.5 Transferability

Based on the home range model with the most support (model 20) I measured external (between areas) and internal (the same areas in different years) transferability for the years and areas available. This resulted in 462 possible combinations of predicted (density estimates derived from external data) and observed (density estimates derived using local data) densities (ptarmigans/per 500x500 grid cell) among the six areas. The landscape scale model with the most support (model 44) was used to measure transferability following the same procedure as above. These two analyses resulted in a total of 924 measurements of internal (n = 128) and external transferability (n = 796). The results unfolded a considerable variation in the measured transferability among areas. This variation was observed for both external transferability and internal transferability at both spatial scales (Figure 6).

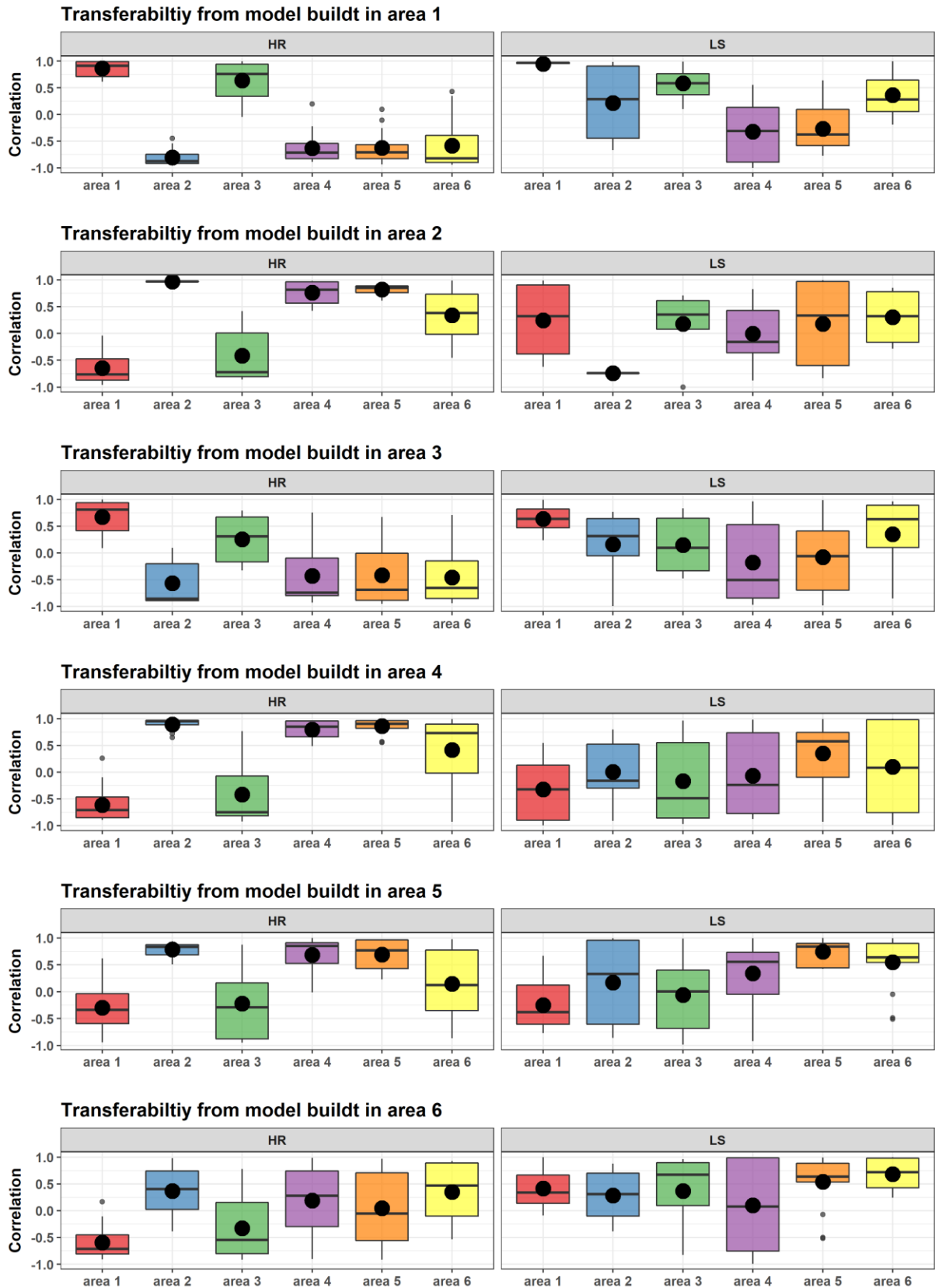


Figure 6: Internal and external transferability (Pearson's correlation) from home range models (HR) to the left and landscape models (LS) to the right, established with local data from the different areas (stated in the headlines). Mean values are included (black dot).

Models established with local data from the six study areas had a low average transferability to other areas (external transferability) at both a landscape scale and home range scale (Figure 7). The highest average external transferability on a home range scale was achieved when using local data from area 2 (mean = 0.16, Figure 7). At a landscape scale the highest average was achieved when using local data from area 6 (mean = 0.35, Figure 6).

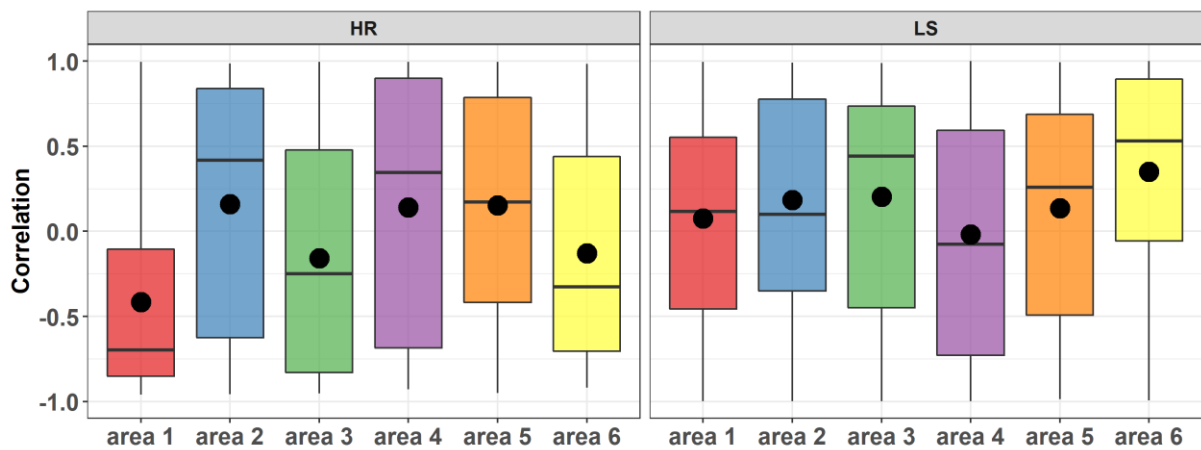


Figure 7: Average external transferability (Pearson's correlation) from focal areas (area 1 to area 6) with home range models (HR) to the left and landscape models (LS) to the right, mean values are included (black dot).

3.6 Factors affecting transferability

To assess factors that affected external model transferability (transferability between areas), I used linear regression with i) distance (km) between the areas and ii) spatial scale (HR and LS) as explanatory variables. In general, I found that the transferability decreased with increasing distance between the study sites at both scales and that the landscape models were more transferable to other areas ($F_{2,793} = 14.27$, $p < 0.05$, $R^2 = 0.03$) (Figure 8a, Appendix J1). Moreover, a regression was fitted to assess how model transferability was affected by an interaction between the explanatory variables i) type of transferability (internal/external) and ii) spatial scale (HR and LS). In general, the internal transferability was higher than external, however, this difference between internal and external was not consistent across spatial scales, as there were indications of a slightly higher internal transferability for home range models compared to landscape models ($F_{3,920} = 34.54$, $p < 0.05$, $R^2 = 0.10$) (appendix J2, Figure 8b).

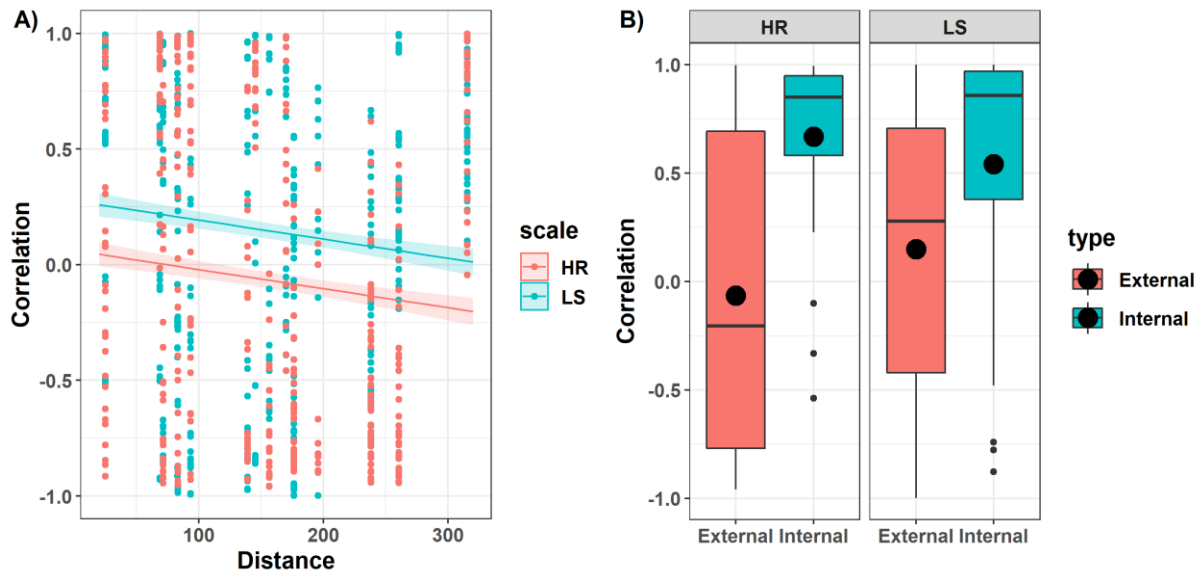


Figure 8: *a)* Scatterplot (data points) with the corresponding relationship (solid line) between distance (km) and transferability (Pearson's correlation) at the spatial scales home range (HR) and landscape (LS), estimated using a regression fitted with 796 data points (Red=home range, blue=Landscape). The transparent fill shows the standard error. *b)* Comparison of the external and internal transferability (Pearson's correlation), at a home range scale (HR) to the left and landscape scale (LS) to the right. Mean values included (black dot).

4.0 Discussion

The main findings in this thesis were: i) covariates at a home range scale had highly heterogeneous relationships with density, both in time and space, ii) covariates at a landscape scale showed less variation in the density relationship compared to home range covariates, iii) models with landscape covariates were more transferable to other areas. iv) models transferred best when predicting density internally within areas across years, and v) external transferability decreased at both spatial scales when the distance between the internal and external area increased. Together, these results are indicative of relatively low transferability of models for density-habitat relationships between areas for willow ptarmigan in a central part of their distributional range. In the remaining of this discussion, I will discuss the validity, potential causes, and implications of my results.

4.1 Variations in covariate effects

The observed heterogeneous habitat-density relationship between the study areas resulted in poor external transferability. Similar issues are often reported from studies focusing on the transferability of predictive habitat suitability models (Yates *et al.*, 2018). In contrast to habitat suitability modeling, few studies have evaluated the transferability of habitat-density models. Nevertheless, some studies are in line with my findings. For instance, Schaub *et al.* (2011) reported that models of territory density for 10 farmland bird species in Switzerland were not transferable in space because of a non-constant habitat-density relationship. Similar issues have also been reported for 11 different farmland birds in Britain (Whittingham *et al.*, 2007). There are at least three possible ecological processes that can be of relevance when discussing explanations of an observed non-consistent habitat-density relationship.

Firstly, one might expect that the observed response in density is correlated with habitat selection, as species presumably select for areas that give benefits to their fitness. A common assumption is therefore that individuals will concentrate in the most favorable habitats, especially if intraspecific competition is limited (Fretwell, 1969; Van Horne, 1983; Fryxell *et al.*, 2014). Habitat selection could therefore explain some of the observed habitat-density relationships in the grid cells covering the study areas. For instance, the negative response in density as a result of an increase in OSF and BSF observed in area 1, coincides with a habitat selection study conducted by Kastedalen *et al.* (2003) in the same area (area 1). He reported that willow ptarmigan avoided large open, dry, and poor areas like heath. Similarly, in subarctic

tundra areas there is evidence for a negative effect in occupancy of willow ptarmigan, as the coverage of willow decreases (Henden *et al.*, 2011; Ehrich *et al.*, 2012). Such avoidance is also supported by Kvasnes *et al.* (2018) who modeled willow ptarmigan habitat suitability across Norway and found that they tend to avoid vegetation with sparse field layer. In general, willow ptarmigan often avoids open areas with sparse vegetation in habitat selection studies. Comparable findings were also observed for the density-habitat relationship at a landscape scale; willow ptarmigan density generally peaked when the grid cells covering the study area were neither completely open, nor completely covered by forests. Such areas are typically close to the treeline. This observed pattern on a landscape scale is in line with well-established literature, stating that ptarmigans are mainly distributed close to the treeline (Kastdalen *et al.*, 2003; Kvasnes *et al.*, 2017; Kvasnes *et al.*, 2018), as a consequence of niche differentiation between ecologically similar grouse species (Swenson & Angelstam, 1993; Pedersen. *et al.*, 2014). Furthermore, the proportion of forest in the cells may be important as shelter habitats, while the proportion of open areas might be used for foraging (Brøseth & Pedersen, 2010).

Secondly, density-dependent responses might create seemingly inconsistent relationships between habitat variables and density, as found in this thesis. When populations show large fluctuations in abundance, spatial and temporal variation in the density-habitat relationship is expected (Kvasnes *et al.*, 2017; Avgar *et al.*, 2020). Studies of several bird populations show evidence of density-dependent habitat relationships. A classic example is a study performed by Brown (1969) which showed that great tits (*Parus major*) primarily nested in woodland habitats in years with low densities, but expanded into hedgerow habitats in years with higher densities. Similarly, Krebs (1971) removed great tits from woodland habits, which resulted in unoccupied space in the woodlands, hedgerow birds then moved to the woodlands. Another example of density dependence for a grouse species is presented by Blomberg *et al.* (2017), who found that female birds had a lower probability to initiate a nest, at high population sizes. Because of density-dependent responses, one can imagine that the habitat-density relationship is dynamic, resulting in poor model transferability when overall density differs between areas used to estimate model parameters and the area for which a prediction is made.

Thirdly, differences in habitat availability between areas might be a reason for the observed variation in the density-habitat relationships. Such spatial variation in habitat use has previously been observed for ptarmigan populations in subarctic tundra areas, where responses in habitat

use in respect to habitat availability (i.e. a functional response in habitat use – see inn Mysterud and Ims (1998)) were reported (Ehrich *et al.*, 2012). Thus, a functional response in habitat use might be the reason for better internal transferability (between years) compared to transferability between areas. For instance, ptarmigan density in the grid cells covering area 1 appeared to be negatively affected when there was an increase in the coverage of OSF and BSF. Interestingly, area 1 also has a low percentage of OSF and BSF available compared to the other five areas. For instance, area 4 has more OSF and BSF available, and positive responses in density were observed when OSF and BSF increased in the grid cells covering area 4 (Figure 3, Figure 4, Appendix A1).

In addition to the three concepts above (habitat selection, density-dependent responses, and functional response in habitat use), it should be emphasized that density in the different grid cells do not necessarily correlate with habitat quality, as a wide range of other ecological mechanisms, like predation, stochastic events, overwinter survival, etc. can affect the density-habitat relationship (Van Horne, 1983). Willow ptarmigans are embedded in a dynamic food web and other mechanisms than the habitat composition are affecting their population dynamics and abundance (Henden *et al.*, 2017). For instance, predation rates can alter the survival rates of grouse species, independently of habitat structure (Marcstrom *et al.*, 1988). Furthermore, the top-down effects of predation on willow ptarmigan populations are assumed to be linked to inter-annual small rodent fluctuations (alternative prey hypothesis) (Hagen, 1989; Breisjøberget *et al.*, 2018), and recent research has shown that such predator mediated interactions increase along a climate harshness gradient (Bowler *et al.*, 2020). Social interactions between individuals should also be considered (Van Horne, 1982, 1983), and there are indications that social behavior and conspecific attraction is affecting settlement decisions in willow ptarmigan (Kvasnes *et al.*, 2015). In addition, harvest management regimes might differ between areas, and can thus cause variation in ptarmigan abundance between years and areas (Sandercock *et al.*, 2011; Kvasnes *et al.*, 2017). The mechanisms above are undoubtedly problematic for model transferability, as other essential covariates than habitat and human disturbance affect the abundance and density of willow ptarmigans in time and space.

It should also be mentioned that the satellite imagery used to develop land cover classifications in SatVeg, stems from 1988-2006, note that this is at least a 10-year difference from the first survey used in this thesis (2016). During this period it is likely that there have been increases

in shrubs and trees as a consequence of climate change and less grazing from domesticated herbivores (Rundqvist *et al.*, 2011). Utilizing remote sensing data with acquisition dates that match the surveys and have a higher spatial resolution, would increase the quality of the landcover classification, and should be considered in further work. For instance, world-view3 images or light detection/ranging technology (LIDAR) could be used, which all have shown promising results regarding habitat analyses (Hyde *et al.*, 2005; Jacquin *et al.*, 2005; Wu *et al.*, 2019). In addition, it could be beneficial to combine remote sensed data and field data which also have shown to increase model transferability (Latif *et al.*, 2016).

4.2 Variations in model transferability

There is no surprise that model transferability varied in time and space, as the habitat-density relationships for ptarmigan is shaped by a variety of ecological and behavioral attributes (see above). This is particularly likely because willow ptarmigan has a short life span and large inter-annual fluctuations in abundance (Andersen *et al.*, 1984; Erikstad, 1985; Fuglei *et al.*, 2019). To my knowledge, there are no previous studies highlighting the problems of poor transferability in abundance/density models for willow ptarmigan as a consequence of spatial and temporal variation in covariate effects. However, a similar study with the use of HDSM by Roach *et al.* (2017) reported problems of model transferability between to areas for clapper rails (*Rallus crepitans*). These birds are using coastal marsh habitat, and transferability was low because of different habitat-use between areas. Latif *et al.* (2016) also reported that varying resource selection patterns likely influenced model transferability for two woodpecker species. In the context of human interventions, Gray *et al.* (2009) presented evidence for poor transferability of a distribution model, because of differences in conservation efforts between areas.

The finding of decreasing transferability at both spatial scales when the distance between the internal and external area increased, are to my knowledge, and as stated by Houlahan *et al.* (2017), not been emphasized with empirical evidence in previous studies related to habitat models. However, Yates *et al.* (2018) discuss that distance does not matter as much as environmental dissimilarity. Dissimilarities in the environment could undoubtedly also be of significance for the relationship between transferability and distance in this thesis. For instance, the transferability among area 1 and 3 seemed in general better compared to several other areas (Figure 6). These two areas also have the longest distance between themselves compared to the

other combinations of the six study areas (Figure 1). In attention to spatial scale, models established with the landscape covariates had an overall better external transferability compared to the home range models. Similar findings concerning model accuracy and precision are common in habitat studies that use more coarsely scaled explanatory variables to predict novel areas (Melles *et al.*, 2003; Fischer *et al.*, 2004; Graf *et al.*, 2005; Loe *et al.*, 2012). This implies that the use of covariates with more coarse spatial scales contributes to better external model transferability.

Another subject that can be addressed, is the possibility that habitat-density relationships are not an appropriate measurement in predictive modeling, especially for a species with large inter-annual fluctuations in abundance. An alternative could be to replace the estimated density with a measurement of the carrying capacity, which does not need to be related to density (Hobbs & Hanley, 1990). To illustrate this, one could imagine a habitat patch with high density as a result of low predation that particular year however, food quantity is too low to sustain the high density, and birth rates decrease, and mortality rates climb until they reach an equilibrium. This equilibrium would be steadier, regardless of the actual density. Hence measurements of the actual carrying capacity for different habitats would be more transferable in time and space.

5.0 Management implications and concluding remarks.

This thesis demonstrates the potential of establishing HDSM`s with data from a nationwide monitoring program (Hønsefuglportalen) to estimate the abundance/density of grouse species in space (Appendix K1 and L1). Spatially explicit predictions of population density can be useful tools in small game harvest management, as the predictions can shed light on how the density is distributed within the management areas in addition to estimates of total abundance within the management area. Areas of high density can function as source areas, thus, withstand a higher local harvest rate, and might be particularly important to protect from land use development. My findings also highlight the large heterogeneity in the habitat-density relationship and model transferability among areas in central Norway. It is therefore in general advisable to be conservative when interpreting predictions done to novel conditions, as the consequences can be profound if using biased models in decision making (Muscatello *et al.*, 2020). Furthermore, local management should strive to use local data, when making decisions concerning willow ptarmigan and density-habitat relationships estimated with HDSM`s.

Literature

- Akaike, H. (1974). A new look at the statistical model identification. *IEEE transactions on automatic control*, 19(6), 716-723.
- Andersen, R., Steen, J. B., & Pedersen, H. C. (1984). Habitat selection in relation to the age of willow grouse *Lagopus l. broods* in central Norway. *Fauna Norvegica*, 7(2), 90-94.
- Avgar, T., Betini, G. S., & Fryxell, J. M. (2020). Habitat selection patterns are density dependent under the ideal free distribution. *Journal of Animal Ecology*, 89(12), 2777-2787.
- Baboo, S. S., & Devi, M. R. (2010). An analysis of different resampling methods in Coimbatore, District. *Global Journal of Computer Science and Technology*, 10(15), 61.
- Blomberg, E. J., Gibson, D., Atamian, M. T., & Sedinger, J. S. (2017). Variable drivers of primary versus secondary nesting; density-dependence and drought effects on greater sage-grouse. *Journal of Avian Biology*, 48(6), 827-836.
- Borchers, D. L., Buckland, S. T., Stephens, W. E., & Zucchini, W. (2002). *Estimating animal abundance: closed populations* (Vol. 13). London: Springer Science & Business Media.
- Bowler, D. E., Kvasnes, M. A. J., Pedersen, H. C., Sandercock, B. K., & Nilsen, E. B. (2020). Impacts of predator-mediated interactions along a climatic gradient on the population dynamics of an alpine bird. *Proceedings of the Royal Society B*, 287(1941), 20202653.
- Breisjøberget, J. I., Odden, M., Wegge, P., Zimmermann, B., & Andreassen, H. (2018). The alternative prey hypothesis revisited: Still valid for willow ptarmigan population dynamics. *PLoS One*, 13(6), e0197289.
- Brown, J. L. (1969). The buffer effect and productivity in tit populations. *The American Naturalist*, 103(932), 347-354.
- Brøseth, H., & Pedersen, H. C. (2010). Disturbance effects of hunting activity in a willow ptarmigan *Lagopus lagopus* population. *Wildlife Biology*, 16(3), 241.
- Buckland, S. T., Anderson, D. R., Burnham, K. P., Laake, J. L., Borchers, D. L., & Thomas, L. (2001). *Introduction to distance sampling: estimating abundance of biological populations*. Oxford (United Kingdom): Oxford Univ. Press.
- Buckland, S. T., Rexstad, E. A., Marques, T. A., & Oedekoven, C. S. (2015). *Distance sampling: methods and applications* (Vol. 431). London: Springer.
- Burt, W. H. (1943). Territoriality and Home Range Concepts as Applied to Mammals. *Journal of Mammalogy*, 24(3), 346-352.
- Chamberlain, D. E., & Fuller, R. (1999). Density-dependent habitat distribution in birds: issues of scale, habitat definition and habitat availability. *Journal of Avian Biology*, 30(4), 427-436.
- Chandler, R. B., Royle, J. A., & King, D. I. (2011). Inference about density and temporary emigration in unmarked populations. *Ecology*, 92(7), 1429-1435.
- Ehrich, D., Henden, J. A., Ims, R. A., Doronina, L. O., Killengren, S. T., Lecomte, N., . . . Sokolov, V. A. (2012). The importance of willow thickets for ptarmigan and hares in shrub tundra: the more the better? *Oecologia*, 168(1), 141-151.

- Erikstad, K. E. (1985). Growth and Survival of Willow Grouse Chicks in Relation to Home Range Size, Brood Movements and Habitat Selection. *Ornis Scandinavica (Scandinavian Journal of Ornithology)*, 16(3), 181-190.
- Fischer, J., Lindenmayer, D. B., & Cowling, A. (2004). The challenge of managing multiple species at multiple scales: reptiles in an Australian grazing landscape. *Journal of applied ecology*, 41(1), 32-44.
- Fiske, I., & Chandler, R. (2011). Unmarked: an R package for fitting hierarchical models of wildlife occurrence and abundance. *Journal of statistical software*, 43(10), 1-23.
- Fretwell, S. D. (1969). On territorial behavior and other factors influencing habitat distribution in birds. *Acta biotheoretica*, 19(1), 45-52.
- Fryxell, J. M., Sinclair, A. R. E., & Caughley, G. (2014). *Wildlife ecology, conservation, and management* (3rd. ed.). Chichester: Wiley Blackwell.
- Fuglei, E., Henden, J. A., Callahan, C. T., Gilg, O., Hansen, J., Ims, R. A., . . . Merizon, R. A. (2019). Circumpolar status of Arctic ptarmigan: population dynamics and trends. *Ambio*, 49(3), 749-761.
- Furnas, B. J., Newton, D. S., Capehart, G. D., & Barrows, C. W. (2019). Hierarchical distance sampling to estimate population sizes of common lizards across a desert ecoregion. *Ecology and evolution*, 9(6), 3046-3058.
- Gill, J. A. (2007). Approaches to measuring the effects of human disturbance on birds. *Ibis*, 149(1), 9-14.
- Gottschalk, T. K., Aue, B., Hotes, S., & Ekschmitt, K. (2011). Influence of grain size on species–habitat models. *Ecological Modelling*, 222(18), 3403-3412.
- Graf, R. F., Bollmann, K., Suter, W., & Bugmann, H. (2005). The importance of spatial scale in habitat models: capercaillie in the Swiss Alps. *Landscape Ecology*, 20(6), 703-717.
- Gray, T. N., Borey, R., Hout, S. K., Chamnan, H., Collar, N., J., & Dolman, P. M. (2009). Generality of models that predict the distribution of species: conservation activity and reduction of model transferability for a threatened bustard. *Conservation Biology*, 23(2), 433-439.
- Guisan, A., & Thuiller, W. (2005). Predicting species distribution: offering more than simple habitat models. *Ecology letters*, 8(9), 993-1009.
- Guisan, A., Thuiller, W., & Zimmermann, N. E. (2017). *Habitat suitability and distribution models: with applications in R*. Cambridge: University Press.
- Guisan, A., & Zimmermann, N. E. (2000). Predictive habitat distribution models in ecology. *Ecological Modelling*, 135(2-3), 147-186.
- Hagen, Y. (1989). *Rovfuglene og viltpleien* (2. ed.). Oslo: Universitetsforlaget.
- Hannon, S., Eason, P., & Martin, K. (1998). *Willow Ptarmigan (Lagopus lagopus)*, version 1.0, in *Birds of the World* (S.M. Billerman, Editor). Ithaca: Cornell Lab of Ornithology.
- Henden, J. A., Ims, R. A., Fuglei, E., & Pedersen, Å. Ø. (2017). Changed Arctic-alpine food web interactions under rapid climate warming: implication for ptarmigan research. *Wildlife Biology*, 2017(SP1).

- Henden, J. A., Ims, R. A., Yoccoz, N. G., & Killengreen, S. T. (2011). Declining willow ptarmigan populations: the role of habitat structure and community dynamics. *Basic and Applied Ecology*, *12*(5), 413-422.
- Hobbs, N. T., & Hanley, T. A. (1990). Habitat evaluation: do use/availability data reflect carrying capacity? *The Journal of Wildlife Management*, *54*(4), 515-522.
- Houlahan, J. E., McKinney, S. T., Anderson, T. M., & McGill, B. J. (2017). The priority of prediction in ecological understanding. *Oikos*, *126*(1), 1-7.
- Hyde, P., Dubayah, R., Peterson, B., Blair, J., Hofton, M., Hunsaker, C., . . . Walker, W. (2005). Mapping forest structure for wildlife habitat analysis using waveform lidar: Validation of montane ecosystems. *Remote Sensing of Environment*, *96*(3-4), 427-437.
- Jacquin, A., Chéret, V., Denux, J.-P., Gay, M., Mitchley, J., & Xofis, P. (2005). Habitat suitability modelling of Capercaillie (*Tetrao urogallus*) using earth observation data. *Journal for Nature Conservation*, *13*(2-3), 161-169.
- Johansen B. E. (2009). Vegetasjonskart for Norge basert på Landsat TM/ETM+ data. *Norut-Tromsø Rapport*, *4*, 86.
- Johansen, B. E., Aarrestad, P. A., & Øien, D. I. (2009). Vegetasjonskart for Norge basert på satellittdata. *Delprosjekt 1: Klasseinndeling og beskrivelse av utskilte vegetasjonstyper*.
- Johnson, D. H. (1980). The Comparison of Usage and Availability Measurements for Evaluating Resource Preference. *Ecology*, *61*(1), 65-71.
- Kastdalen, L., Pedersen, H., Fjone, G., & Andreassen, H. (2003). *Combining resource selection functions and distance sampling: an example with willow ptarmigan*. Paper presented at the Resource selection methods and application. Western EcoSystems Technology, Cheyenne, Wyoming, USA.
- Kerbs, C. (1972). *Ecology: the experimental analysis of distribution and abundance*. New York: Harper and Row
- Krebs, J. R. (1971). Territory and breeding density in the Great Tit, *Parus major* L. *Ecology*, *52*(1), 2-22.
- Kvasnes, M. A. J., Pedersen, H. C., Kjøsberg, M., Rød-Eriksen, L., Eriksen, L. F., Bowler, D., . . . Moa, P. F. (2019). Hønsefuglportalen. Oppsummering av drift og utvikling i perioden 2013-2018. *NINA rapport 1664*.
- Kvasnes, M. A. J., Pedersen, H. C., & Nilsen, E. B. (2018). Quantifying suitable late summer brood habitats for willow ptarmigan in Norway. *BMC Ecology*, *18*(1), 41.
- Kvasnes, M. A. J., Pedersen, H. C., Solvang, H., Storaas, T., & Nilsen, E. B. (2015). Spatial distribution and settlement strategies in willow ptarmigan. *Population Ecology*, *57*(1), 151-161.
- Kvasnes, M. A. J., Pedersen, H. C., Storaas, T., & Nilsen, E. B. (2017). Vegetation type and demography of low density willow ptarmigan populations. *The Journal of Wildlife Management*, *81*(1), 174-181.
- Latif, Q. S., Saab, V. A., Hollenbeck, J. P., & Dudley, J. G. (2016). Transferability of habitat suitability models for nesting woodpeckers associated with wildfire. *The Condor: Ornithological Applications*, *118*(4), 766-790.

- Le Moullec, M., Pedersen, Å. Ø., Yoccoz, N. G., Aanes, R., Tufto, J., & Hansen, B. B. (2017). Ungulate population monitoring in an open tundra landscape: distance sampling versus total counts. *Wildlife Biology*, 2017(4).
- Lens, L., Van Dongen, S., Norris, K., Githiru, M., & Matthysen, E. (2002). Avian persistence in fragmented rainforest. *Science*, 298(5596), 1236-1238.
- Lobo, J. M., Jiménez-Valverde, A., & Hortal, J. (2010). The uncertain nature of absences and their importance in species distribution modelling. *Ecography*, 33(1), 103-114.
- Loe, L. E., Bonenfant, C., Meisingset, E. L., & Mysterud, A. (2012). Effects of spatial scale and sample size in GPS-based species distribution models: are the best models trivial for red deer management? *European Journal of Wildlife Research*, 58(1), 195-203.
- Manzoor, S. A., Griffiths, G., & Lukac, M. (2018). Species distribution model transferability and model grain size—finer may not always be better. *Scientific reports*, 8(1), 1-9.
- Marcstrom, V., Kenward, R., & Engren, E. (1988). The impact of predation on boreal tetraonids during vole cycles: an experimental study. *The Journal of animal ecology*, 57(3), 859-872.
- Mayer, D., & Butler, D. (1993). Statistical validation. *Ecological Modelling*, 68(1-2), 21-32.
- Mayor, S. J., Schneider, D. C., Schaefer, J. A., & Mahoney, S. P. (2009). Habitat selection at multiple scales. *Ecoscience*, 16(2), 238-247.
- Melles, S., Glenn, S., & Martin, K. (2003). Urban bird diversity and landscape complexity: species–environment associations along a multiscale habitat gradient. *Conservation Ecology*, 7(1).
- Miller, D. L., Burt, M. L., Rexstad, E. A., & Thomas, L. (2013). Spatial models for distance sampling data: recent developments and future directions. *Methods in ecology and evolution*, 4(11), 1001-1010.
- Moen, A., Odland, A., & Lillethun, A. (1998). *Vegetasjon*. Hønefoss: Norges geografiske oppmåling.
- Mouquet, N., Lagadeuc, Y., Devictor, V., Doyen, L., Duputié, A., Eveillard, D., . . . Huneman, P. (2015). Predictive ecology in a changing world. *Journal of applied ecology*, 52(5), 1293-1310.
- Muscatello, A., Elith, J., & Kujala, H. (2020). How decisions about fitting species distribution models affect conservation outcomes. *Conservation Biology*, 0(0), 1-12.
- Myneni, R. B., Hall, F. G., Sellers, P. J., & Marshak, A. L. (1995). The interpretation of spectral vegetation indexes. *IEEE Transactions on Geoscience and Remote Sensing*, 33(2), 481-486.
- Myrberget, S. (1988). Demography of an island population of willow ptarmigan in northern Norway. *Adaptive strategies and population ecology of northern grouse*, 379-419.
- Mysterud, A., & Ims, R. A. (1998). Functional responses in habitat use: Availability influences relative use in trade-off situations. *Ecology*, 79(4), 1435-1441.
- Nilsen, E. B., Vang, R., & Breisjøberget, J. (2020 b). Tetraonid line transect surveys from Norway: Data from Statskog. Version 1.6. *Norwegian Institute for Nature Research. Sampling event dataset* doi: <https://doi.org/10.15468/q2ehlk> accessed via GBIF.org on 2020-11-26.
- Nilsen, E. B., Vang, R., Kjøsberg, M., & Kvasnes, M. A. J. (2020 a). Tetraonid line transect surveys from Norway: Data from Fjellstyrene. Version 1.3. *Norwegian Institute for Nature Research*.

Sampling event dataset. doi:<https://doi.org/10.15468/975ski> accessed via GBIF.org on 2020-10-12.

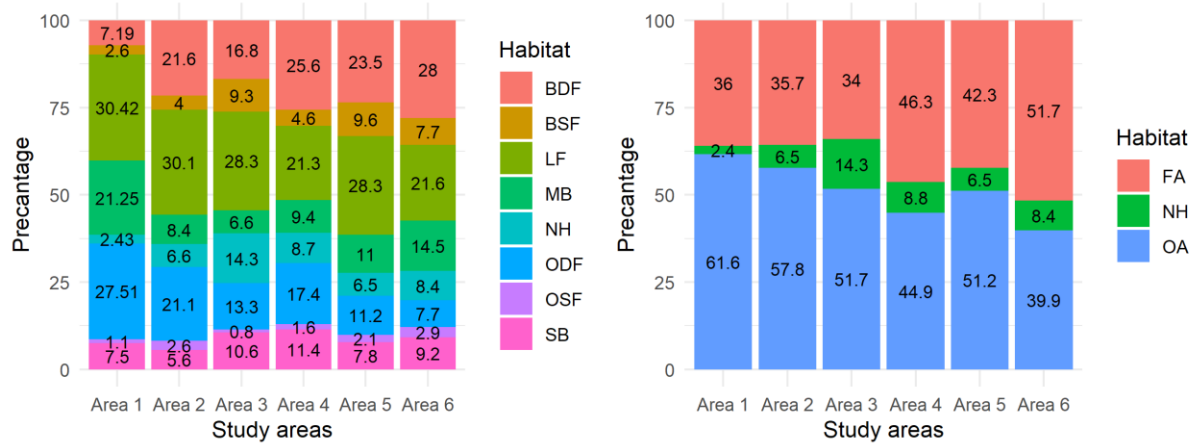
- Orpin, C. G., Mathiesen, S. D., Greenwood, y., & Blix, A. S. (1985). Seasonal changes in the ruminal microflora of the high-arctic Svalbard reindeer (*Rangifer tarandus platyrhynchus*). *Applied and Environmental Microbiology*, *50*(1), 144-151.
- Pedersen, & Storaas, T. (2013). *Rypeforvaltning : Rypeforvaltningsprosjektet 2006-2011 og veien videre*. Oslo: Cappelen Damm akademisk.
- Pedersen, H. C., Steen, H., Kastdalen, L., Brøseth, H., Ims, R., Svendsen, W., & Yoccoz, N. (2004). Weak compensation of harvest despite strong density-dependent growth in willow ptarmigan. *Proceedings of the Royal Society of London. Series B: Biological Sciences*, *271*(1537), 381-385.
- Pedersen, Å. Ø., Blanchet, M.-A., Hörnell-Willebrand, M., Jepsen, J. U., Biuw, M., & Fuglei, E. (2014). Rock Ptarmigan (*Lagopus muta*) breeding habitat use in northern Sweden. *Journal of Ornithology*, *155*(1), 195-209.
- Pettorelli, N., Vik, J. O., Mysterud, A., Gaillard, J.-M., Tucker, C. J., & Stenseth, N. C. (2005). Using the satellite-derived NDVI to assess ecological responses to environmental change. *Trends in ecology & evolution*, *20*(9), 503-510.
- Potapov, R. d. L., & Sale, R. (2013). *Grouse of the world*. United kingdom New Holland Publishers.
- R Core Team. (2021). A language and environment for statistical computing. Vienna, Austria. Retrieved from <https://www.R-project.org/>
- Roach, N. S., Hunter, E. A., Nibbelink, N. P., & Barrett, K. (2017). Poor transferability of a distribution model for a widespread coastal marsh bird in the southeastern United States. *Ecosphere*, *8*(3), e01715.
- Royle, J. A., Dawson, D. K., & Bates, S. (2004). Modeling abundance effects in distance sampling. *Ecology*, *85*(6), 1591-1597.
- Rundqvist, S., Hedenås, H., Sandström, A., Emanuelsson, U., Eriksson, H., Jonasson, C., & Callaghan, T. V. (2011). Tree and shrub expansion over the past 34 years at the tree-line near Abisko, Sweden. *Ambio*, *40*(6), 683.
- Sandercock, B. K., Nilsen, E. B., Brøseth, H., & Pedersen, H. C. (2011). Is hunting mortality additive or compensatory to natural mortality? Effects of experimental harvest on the survival and cause-specific mortality of willow ptarmigan. *Journal of Animal Ecology*, *80*(1), 244-258.
- Schaub, M., Kéry, M., Birrer, S., Rudin, M., & Jenni, L. (2011). Habitat-density associations are not geographically transferable in Swiss farmland birds. *Ecography*, *34*(4), 693-704.
- Schwarz, C. J., & Seber, G. A. (1999). Estimating animal abundance: review III. *Statistical Science*, *14*(4), 427-456.
- Seber, G. A. (1986). A review of estimating animal abundance. *Biometrics*, *42*(2), 267-292.
- Sequeira, A. M., Bouchet, P. J., Yates, K. L., Mengersen, K., & Caley, M. J. (2018). Transferring biodiversity models for conservation: opportunities and challenges. *Methods in ecology and evolution*, *9*(5), 1250-1264.

- Sillett, T. S., Chandler, R. B., Royle, J. A., Kéry, M., & Morrison, S. A. (2012). Hierarchical distance-sampling models to estimate population size and habitat-specific abundance of an island endemic. *Ecological Applications*, 22(7), 1997-2006.
- Steen, H., & Erikstad, K. E. (1996). Sensitivity of willow grouse *Lagopus lagopus* population dynamics to variations in demographic parameters. *Wildlife Biology*, 2(3), 27-35.
- Steen, J. B., Chr, H., Erikstad, K. E., Hansen, K. B., Høydal, K., & Størdal, A. (1985). The significance of cock territories in willow ptarmigan. *Ornis Scandinavica*, 16(4), 277-282.
- Swenson, J. E., & Angelstam, P. (1993). Habitat separation by sympatric forest grouse in Fennoscandia in relation to boreal forest succession. *Canadian Journal of Zoology*, 71(7), 1303-1310.
- Talbot, L. M., & Stewart, D. (1964). First wildlife census of the entire Serengeti-Mara region, East Africa. *The Journal of Wildlife Management*, 28(4), 815-827.
- Turner, M. G., Gardner, R. H., O'neill, R. V., & O'Neill, R. V. (2001). *Landscape ecology in theory and practice* (Vol. 401). New York: Springer.
- Urban, M. C., Bocedi, G., Hendry, A. P., Mihoub, J.-B., Pe'er, G., Singer, A., . . . Godsoe, W. (2016). Improving the forecast for biodiversity under climate change. *Science*, 353(6304), 1113-1124.
- Van Horne, B. (1982). Niches of adult and juvenile deer mice (*Peromyscus maniculatus*) in seral stages of coniferous forest. *Ecology*, 63(4), 992-1003.
- Van Horne, B. (1983). Density as a misleading indicator of habitat quality. *The Journal of Wildlife Management*, 47(4), 893-901.
- Warren, P., & Baines, D. (2011). Evaluation of the distance sampling technique to survey red grouse *Lagopus lagopus scoticus* on moors in northern England. *Wildlife Biology*, 17(2), 135-142.
- Whittingham, M. J., Krebs, J. R., Swetnam, R. D., Vickery, J. A., Wilson, J. D., & Freckleton, R. P. (2007). Should conservation strategies consider spatial generality? Farmland birds show regional not national patterns of habitat association. *Ecology letters*, 10(1), 25-35.
- Williams, B. K., Nichols, J. D., & Conroy, M. J. (2002). *Analysis and management of animal populations*. San Diego: Academic Press.
- Wilson, G. J., & Delahay, R. J. (2001). A review of methods to estimate the abundance of terrestrial carnivores using field signs and observation. *Wildlife Research*, 28(2), 151-164.
- Wisz, M. S., Pottier, J., Kissling, W. D., Pellissier, L., Lenoir, J., Damgaard, C. F., . . . Guisan, A. (2013). The role of biotic interactions in shaping distributions and realised assemblages of species: implications for species distribution modelling. *Biological reviews*, 88(1), 15-30.
- Woodward, F. I., & Williams, B. (1987). Climate and plant distribution at global and local scales. *Vegetatio*, 69(1), 189-197.
- Wu, H., Levin, N., Seabrook, L., Moore, B. D., & McAlpine, C. (2019). Mapping foliar nutrition using WorldView-3 and WorldView-2 to assess Koala habitat suitability. *Remote Sensing*, 11(3), 215.
- Yates, K. L., Bouchet, P. J., Caley, M. J., Mengersen, K., Randin, C. F., Parnell, S., . . . Barbosa, A. M. (2018). Outstanding challenges in the transferability of ecological models. *Trends in ecology & evolution*, 33(10), 790-802.

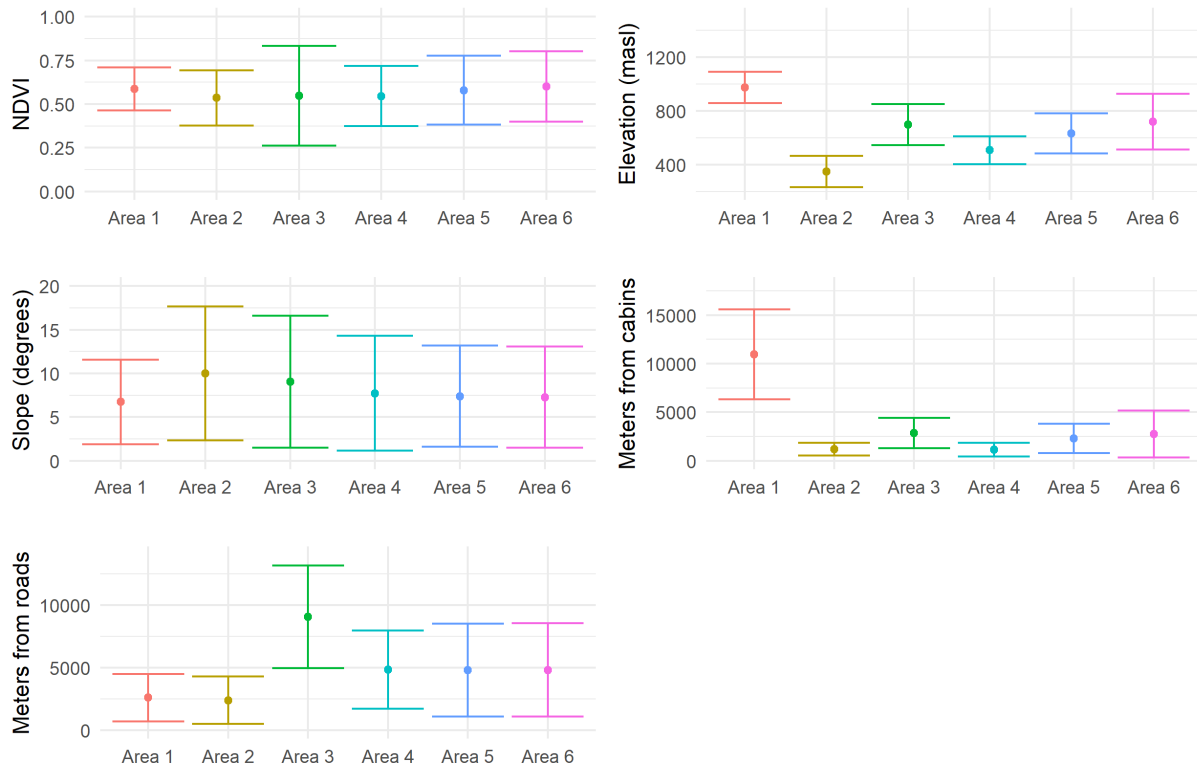
Appendices

Appendix A

Appendix A1: The percentage (labels) of different landcover (habitat) in the six different study areas. To the left are landcover types on a home range scale, to the right landscape scale. (BDF = bogs with dense field layer, BSF = bogs with sparse field layer, LF = low land forest, MB = mountain birch, ODF = open areas with dense field layer, OSF = Open areas with sparse field layer, SB = snow bed vegetation, FA = forested areas, OA = open areas, NH = non-habitat). See chapter 2.4 and appendix B for further details regarding the landcover types.

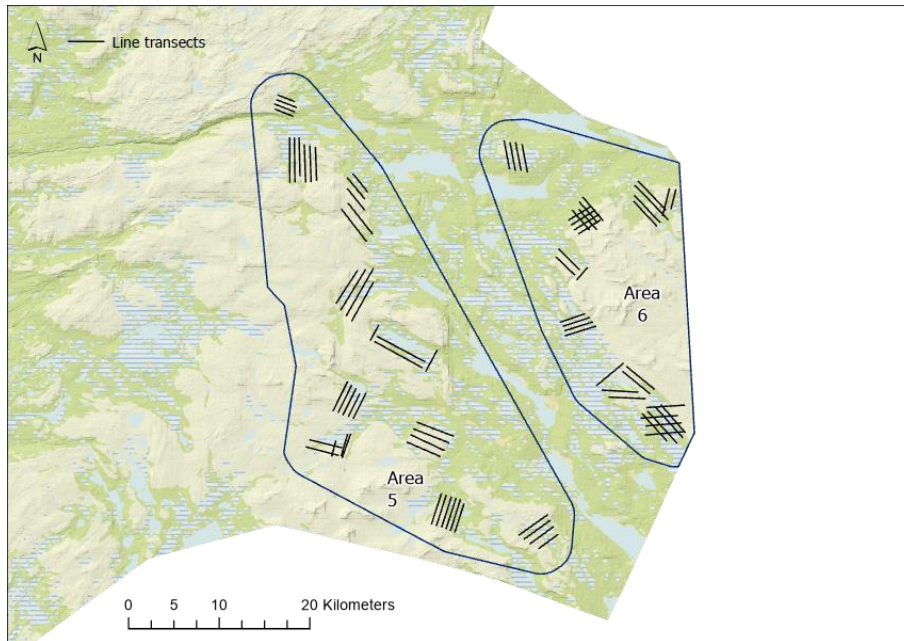


Appendix A2: Plots presenting the mean value of five different environmental covariates in the six study areas with error bars (\pm standard deviation). (NDVI=normalized vegetation index, masl = meters above sea level).

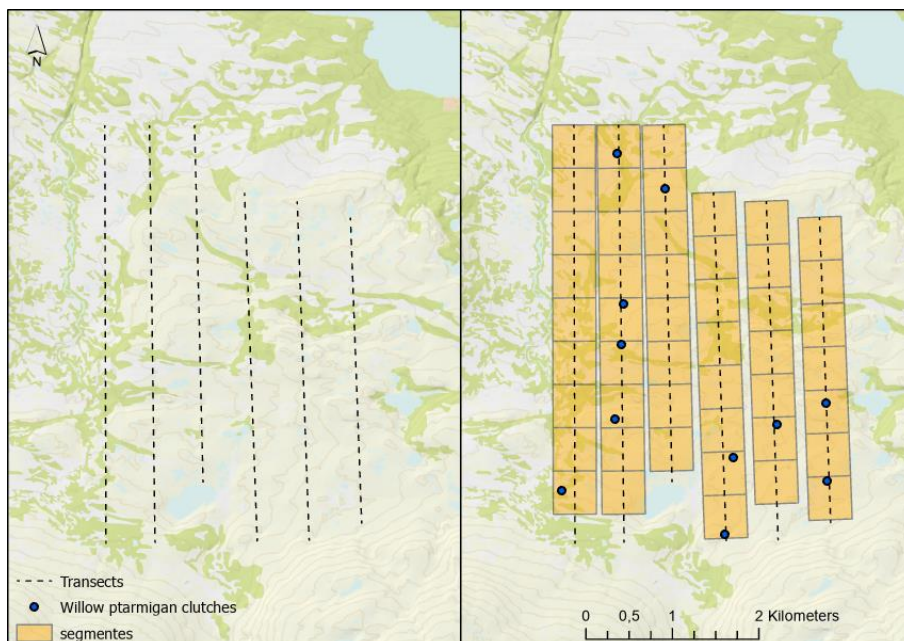


Appendix B

Appendix B1: Example of the distribution and position of transects in study area 5 and 6, used in distance sampling surveys in the years 2019-2020.



Appendix B2: Line transects (left), and line transects with 500 x 500m segments. From study area 5. The GPS occurrences of willow ptarmigan clutches are from the distance sampling survey done in 2019.



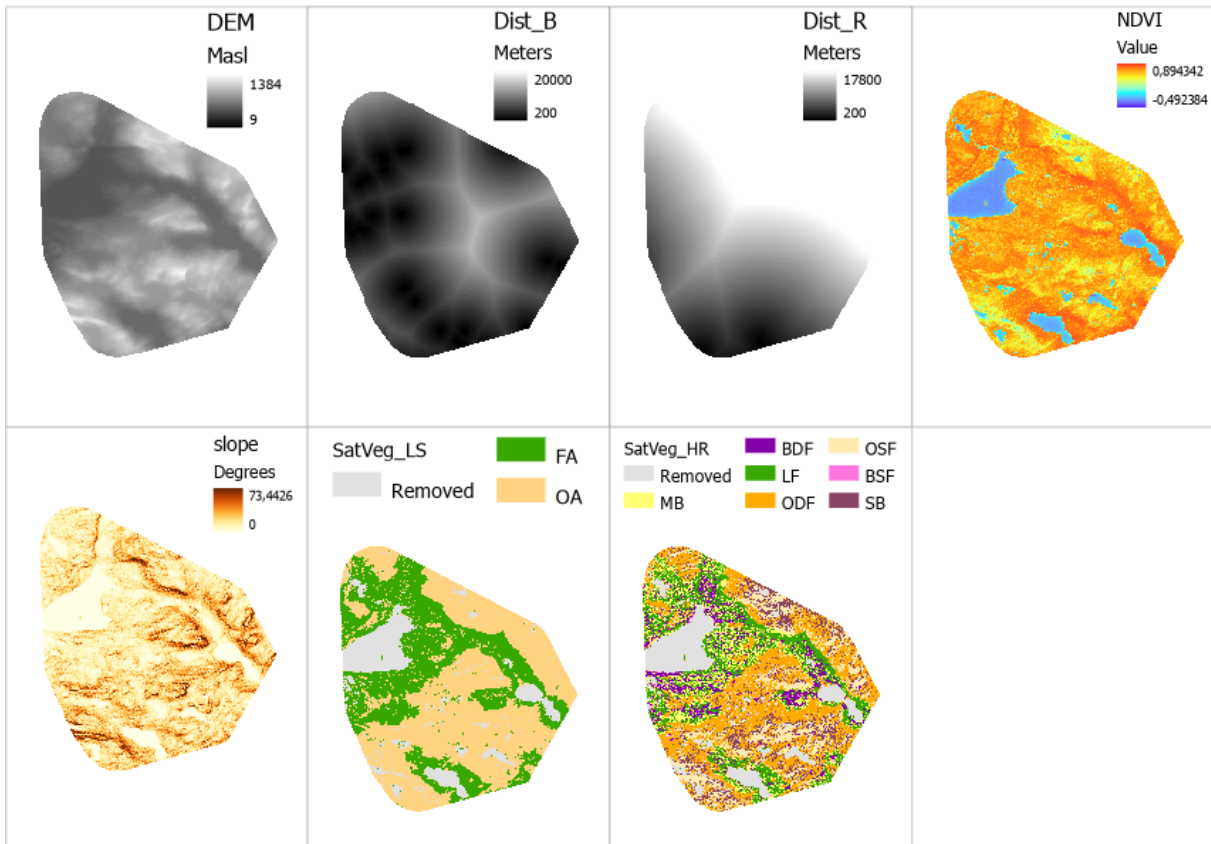
Appendix C

Appendix C1: The original 25 vegetation types classified in the Satveg dataset with the original raster values (Johansen et al., 2009). And an overview of which of the original classes included in the two new reclassified raster datasets. Similar classifications can be found in Kvasnes et al. (2017) and Brøseth and Pedersen (2010).

Original categories	Home range scale	Landscape scale
<i>Bilberry-low fern birch forests (6)</i> <i>Crowberry birch forests (7)</i> <i>Lichen-rich birch forest (8)</i>	<i>Mountain birch forests (MB)</i>	<i>Forested vegetation (FV)</i>
<i>Ombrotrophic bog and low-grown lawn vegetation (9)</i> <i>Tall-grown lawn vegetation (10)</i>	<i>Bogs with dense field layer (BDF)</i>	
<i>Coniferous forest-dense canopy layer (1)</i> <i>Coniferous and mixed forest- open canopy layer (2)</i> <i>Lichen riche pine forest (3)</i> <i>Low herb forest and broad-leaved deciduous forest (4)</i> <i>Low herb-tall fern deciduous forest (5)</i>	<i>Lowland/boreal forest (LF)</i>	
<i>Heather- and grass-rich early snow patch community (16)</i> <i>Fresh heather and dwarf -shrub communities (17)</i>	<i>Open areas with dense field layer (ODF)</i>	
<i>Exposed alpine ridges, scree, and rock complex (12)</i> <i>Graminoid alpine ridge vegetation (13)</i> <i>Heather-rich alpine ridge vegetation (14)</i> <i>Lichen rich heathland (15)</i> <i>Herb-rich meadows (18)</i>	<i>Open areas with sparse field layer (OSF)</i>	
<i>Wet mire, sedge swamps and reed beds (11)</i>	<i>Swamps and bogs with sparse field layer (BSF)</i>	
<i>Grass and dwarf willow snow-patch vegetation (19)</i> <i>Bryophyta late snow patch vegetation (20)</i>	<i>Snowbeds (SB)</i>	
<i>Glacier, snow, and wet snow-patch vegetation (21)</i> <i>Water (22)</i> <i>Agricultural areas (23)</i> <i>Cities and developed areas (24)</i> <i>Unclassified and shadow affected areas (25)</i>	<i>Removed from the dataset</i>	

Appendix D

Appendix D1: Example of all covariates as raster maps (30 x 30m) used to extract mean values and percentage land cover to the unique segments in area 3 (Dist_b = distance to buildings, Dist_r = distance to roads, HR=home range scale, LS=landscape scale).

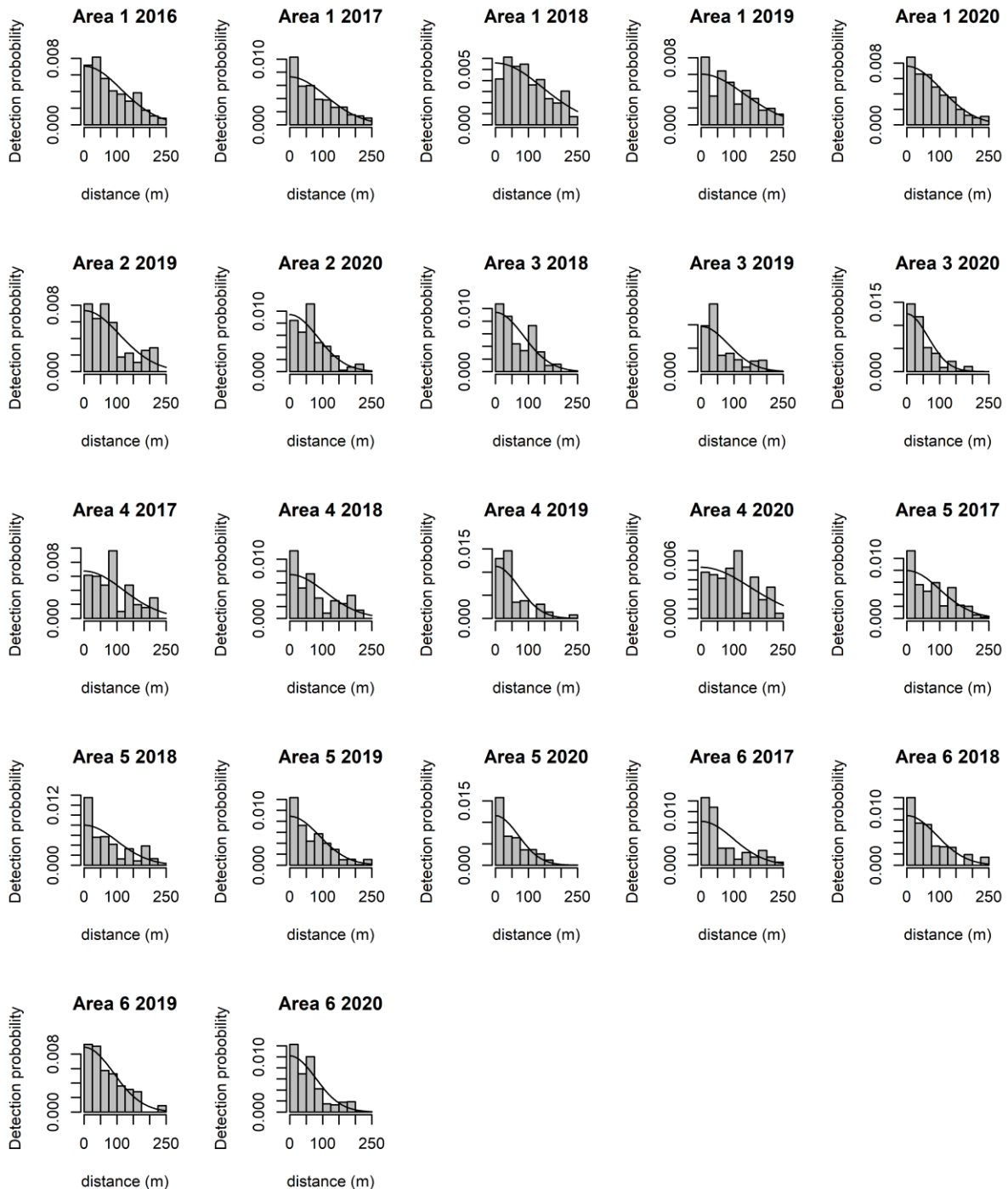


Appendix D2: Spearman's rank correlation matrix, between covariates on a home range scale. And an independent correlation matrix for the landscape scale (FA and OA). Values below -0.55 and above 0.55 are highlighted (Dist b = distance to buildings, Dist r = distance to roads) and not used together to model the density parameter.

	NDVI	DEM	slope	Dist_b	Dist_r	OSF	ODF	BDF	BSF	MB	LF	SB	OA	FA
NDVI	-	0.16	0.22	-0.10	0.14	-0.35	-0.42	0.18	0.12	0.57	0.47	-0.31	-	-
DEM	0.16	-	0.02	0.64	-0.31	0.23	-0.01	0.13	-0.16	-0.15	-0.31	-0.16	-	-
slope	0.22	0.02	-	-0.02	-0.03	0.21	0.16	-0.37	-0.41	-0.07	-0.04	0.13	-	-
Dist_b	-0.10	0.64	-0.02	-	-0.18	0.31	0.11	0.13	-0.18	-0.23	-0.45	-0.09	-	-
Dist_r	0.14	-0.31	-0.03	-0.18	-	-0.18	0.08	-0.22	0.02	0.15	0.11	0.24	-	-
OSF	-0.35	0.23	0.21	0.31	-0.18	-	0.32	-0.25	-0.40	-0.59	-0.62	0.11	-	-
ODF	-0.42	-0.01	0.16	0.11	0.08	0.32	-	-0.61	-0.41	-0.58	-0.53	0.59	-	-
BDF	0.18	0.13	-0.37	0.13	-0.22	-0.25	-0.61	-	0.51	0.27	0.12	-0.59	-	-
BSF	0.12	-0.16	-0.41	-0.18	0.02	-0.40	-0.41	0.51	-	0.30	0.32	-0.28	-	-
MB	0.57	-0.15	-0.07	-0.23	0.15	-0.59	-0.58	0.27	0.30	-	0.76	-0.34	-	-
LF	0.47	-0.31	-0.04	-0.45	0.11	-0.62	-0.53	0.12	0.32	0.76	-	-0.25	-	-
SB	-0.31	-0.16	0.13	-0.09	0.24	0.11	0.59	-0.59	-0.28	-0.34	-0.25	-	-	-
OA	-	-	-	-	-	-	-	-	-	-	-	-	-	-0.99
FA	-	-	-	-	-	-	-	-	-	-	-	-	-0.99	-

Appendix E

Appendix E1: The number of observations of ptarmigan clutches grouped in 25m distance intervals from the transect line (histogram). A half-normal detection function (solid line) is included in the plots, with the detection probability on the y-axes.



Appendix F

Appendix F1: Akaike information criterion (AIC) for all model candidates. Covariates affecting ptarmigan density (λ) and covariates affecting the shape parameter for a half-normal detection function (σ). (FA = forested areas, OA = open areas, OSF = open areas with sparse field layer, ODF = open areas with dense field layer, BSF = bogs with sparse field layer, LF = lowland forest, NDVI = Normalized difference vegetation index. The mean absolute error (MAE) with standard deviation (SD) from the 3-folded cross-validation procedure is also included.

Model	Covariates	AIC	MAE \pm SD
Home range models			
Model 20:	ODF(σ) ~ OSF + BSF(λ)	3713.34	0.32 \pm 0.03
Model 16:	ODF(σ) ~ OSF + slope ² (λ)	3719.90	0.32 \pm 0.01
Model 19:	ODF(σ) ~ OSF + BDF(λ)	3720.76	0.31 \pm 0.04
Model 28:	ODF(σ) ~ OSF ² (λ)	3722.04	0.34 \pm 0.02
Model 4:	ODF(σ) ~ OSF(λ)	3722.10	0.31 \pm 0.00
Model 21:	ODF(σ) ~ ODF + OSF(λ)	3722.54	0.31 \pm 0.02
Model 26:	ODF(σ) ~ BSF + MB + LF(λ)	3734.19	0.32 \pm 0.01
Model 25:	ODF(σ) ~ BDF + MB + LF(λ)	3739.12	0.32 \pm 0.02
Model 23:	ODF(σ) ~ ODF + LF(λ)	3739.62	0.31 \pm 0.03
Model 8:	ODF(σ) ~ LF(λ)	3739.64	0.32 \pm 0.01
Model 30:	ODF(σ) ~ slope ² (λ)	3745.57	0.32 \pm 0.02
Model 18:	ODF(σ) ~ NDVI + slope ² (λ)	3746.35	0.32 \pm 0.01
Model 17:	ODF(σ) ~ ODF + slope ² (λ)	3746.81	0.32 \pm 0.02
Model 11:	ODF(σ) ~ slope(λ)	3747.74	0.32 \pm 0.00
Model 7:	ODF(σ) ~ MB(λ)	3750.22	0.32 \pm 0.03
Model 2:	ODF(σ) ~ NDVI(λ)	3752.85	0.32 \pm 0.02
Model 29:	ODF(σ) ~ NDVI ² (λ)	3754.85	0.32 \pm 0.03
Model 24:	ODF(σ) ~ ODF + SB(λ)	3754.85	0.32 \pm 0.01
Model 27:	ODF(σ) ~ ODF ² (λ)	3757.73	0.32 \pm 0.02
Model 9:	ODF(σ) ~ SB(λ)	3757.98	0.32 \pm 0.00
Model 22:	ODF(σ) ~ ODF + BSF(λ)	3758.24	0.32 \pm 0.02
Model 31:	ODF(σ) ~ meters above sea level ² (λ)	3758.48	0.32 \pm 0.01
Model 5:	ODF(σ) ~ BSF(λ)	3760.14	0.31 \pm 0.00
Model 1:	(σ) ~ (λ)	3760.84	0.32 \pm 0.01
Model 3:	ODF(σ) ~ ODF(λ)	3760.85	0.32 \pm 0.01
Model 6:	ODF(σ) ~ BDF(λ)	3762.34	0.32 \pm 0.02
Model 40:	ODF(σ) ~ slope + meters above sea level (λ)	3785.36	0.32 \pm 0.03
Model 10:	ODF(σ) ~ meters above sea level (λ)	3886.89	0.32 \pm 0.02
Model 34:	ODF(σ) ~ OSF + BDF + distance to buildings(λ)	3911.97	0.30 \pm 0.07
Model 38:	ODF(σ) ~ ODF + distance to buildings(λ)	4009.74	0.31 \pm 0.06
Model 33:	ODF(σ) ~ OSF + BSF + distance to buildings(λ)	4015.83	0.28 \pm 0.04
Model 37:	ODF(σ) ~ OSF + distance to buildings(λ)	4016.93	0.32 \pm 0.06
Model 12:	ODF(σ) ~ distance to buildings(λ)	4109.93	0.25 \pm 0.07
Model 14:	ODF(σ) ~ NDVI + distance to buildings(λ)	4111.93	0.24 \pm 0.08
Model 13:	ODF(σ) ~ distance to roads(λ)	5080.74	0.19 \pm 0.03
Model 15:	ODF(σ) ~ NDVI + distance to roads(λ)	5082.74	0.19 \pm 0.03
Model 36:	ODF(σ) ~ OSF + distance to roads(λ)	5082.74	0.19 \pm 0.02
Model 39:	ODF(σ) ~ ODF + distance to roads(λ)	5082.74	0.19 \pm 0.05
Model 32:	ODF(σ) ~ OSF + BSF + distance to roads(λ)	5084.74	0.19 \pm 0.02
Model 35:	ODF(σ) ~ OSF + BDF + distance to roads(λ)	5084.74	0.19 \pm 0.03
Landscape models			
Model 44:	FA(σ) ~ FA ² (λ)	3734.08	0.32 \pm 0.01
Model 43:	FA(σ) ~ OA ² (λ)	3745.11	0.32 \pm 0.01
Model 41:	FA(σ) ~ OA (λ)	3754.33	0.32 \pm 0.02
Model 42:	FA(σ) ~ FA (λ)	3754.98	0.32 \pm 0.02
Model 1:	(σ) ~ (λ)	3760.84	0.32 \pm 0.01

Appendix G

There were no substantial indications that the half normal-detection function was dependent on the coverage of open areas with dense field layer (Appendix G1), or forested areas (Appendix G2). Because parameter estimates were close to zero, meaning that the detection curve does not change considerably as the coverage of the environmental covariate's changes, still there were some exceptions (e.g., Area 1 in 2019).

Appendix G1: Parameter estimates on a log-scale (with p-values in parentheses) from the home range models fitted with local data from the six study areas. Detectability (σ) as a function of the percentage coverage of open areas with dense field layer (ODF).

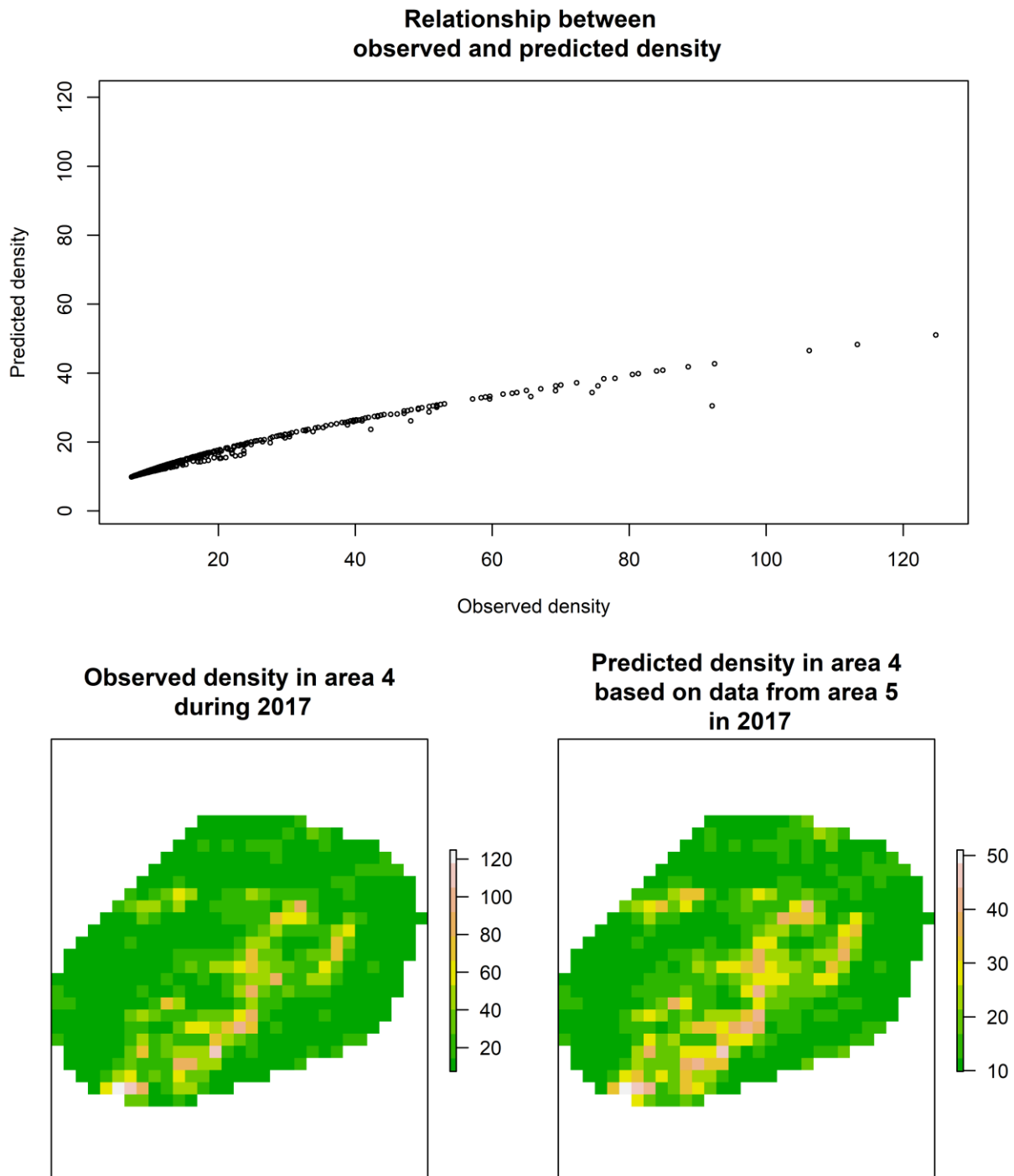
	Area 1	Area 2	Area 3	Area 4	Area 5	Area 6
2016						
ODF (σ):	0.001 ($p = 0.49$)	n/a	n/a	n/a	n/a	n/a
2017						
ODF (σ):	- 0.001 ($p = 0.25$)	n/a	0.030 ($p < 0.05$)	n/a	- 0.001 ($p = 0.51$)	0.004 ($p = 0.25$)
2018						
ODF (σ):	0.007 ($p < 0.05$)	n/a	0.013 ($p < 0.05$)	0.001 ($p = 0.47$)	0.002 ($p < 0.01$)	- 0.005 ($p < 0.01$)
2019						
ODF (σ):	0.399 ($p < 0.05$)	0.017 ($p < 0.05$)	0.005 ($p = 0.01$)	0.01 ($p = 0.07$)	0.001 ($p = 0.07$)	0.012 ($p < 0.01$)
2020						
ODF (σ):	0.002 ($p = 0.06$)	0.015 ($p < 0.05$)	- 0.004 ($p = 0.01$)	- 0.004 ($p < 0.05$)	0.004 ($p < 0.05$)	0.006 ($p < 0.05$)

Appendix G2: Parameter estimates on a log-scale (with p-values in parentheses) from the landscape models fitted with local data from the six study areas. Detectability (σ) as a function of the percentage coverage of forested areas (FA).

	Area 1	Area 2	Area 3	Area 4	Area 5	Area 6
2016						
FA (σ):	0.257 ($p < 0.01$)	n/a	n/a	n/a	n/a	n/a
2017						
FA (σ):	0.002 ($p = 0.01$)	n/a	- 0.005 ($p = 0.24$)	n/a	0.002 ($p = 0.88$)	0.004 ($p = 0.02$)
2018						
FA (σ):	0.004 ($p = 0.01$)	n/a	- 0.00005 ($p = 0.99$)	0.0003 ($p = 0.85$)	0.002 ($p = 0.02$)	0.014 ($p < 0.01$)
2019						
FA (σ):	- 0.003 ($p = 0.01$)	- 0.021 ($p < 0.01$)	0.0006 ($p = 0.75$)	0.001 ($p = 0.37$)	0.0006 ($p = 0.51$)	- 0.009 ($p < 0.01$)
2020						
FA (σ):	0.002 ($p = 0.14$)	- 0.003 ($p = 0.32$)	0.006 ($p < 0.05$)	0.331 ($p < 0.05$)	- 0.001 ($p = 0.76$)	- 0.002 ($p = 0.06$)

Appendix H

Appendix H1: Example of raster maps presenting observed density in 500 x 500m grid cells covering area 4 estimated with local data in area 4 during 2017 and predicted density in 500 x 500 m grid cells covering area 4 based on a model established with non-local data, from area 5 in 2017. And a plot of the relationship between the predicted and the observed density from the distribution maps.



Appendix I

Appendix I1) Parameter estimates on a log-scale from the HDSM (hierarchical distance sampling model) established with home range covariates with the most support among the fitted models established with data from the reference area (area 5 in 2017).

Formula: $ODF(\sigma) \sim OSF + BSF(\lambda)$

<u>Density (σ)</u>				
	Estimate	SE	Z	P(> z)
(intercept)	2.2872	0.07545	30.31	7.89e-202
OSF	0.0172	0.00229	7.54	4.60e-14
BSF	0.0381	0.01057	3.61	3.12e-04

<u>Detection (λ)</u>				
	Estimate	SE	Z	P(> z)
(intercept)	4.632194	0.05543	83.571	0.000
ODF	-0.000672	0.00104	-0.647	0.518

Appendix I2) Parameter estimates on a log-scale from the HDSM (hierarchical distance sampling model) established with landscape covariates with the most support among the fitted models established with data from the reference area (area 5 in 2017).

Formula: $FA(\sigma) \sim Poly(FA,2)(\lambda)$

<u>Density (σ)</u>				
	Estimate	SE	Z	P(> z)
(intercept)	2.55	0.589	43.32	0.00e+00
Poly (FA,2)1	-3.64	1.0725	43.32	6.82e-04
Poly (FA,2)2	-3.76	0.7883	-4.77	1.81e-06

<u>Detection (λ)</u>				
	Estimate	SE	Z	P(> z)
(intercept)	4.53717	0.05375	84.41	0.0000
FA	0.00192	0.00112	1.71	0.0877

Appendix J

Appendix J1) Parameter estimates for the linear regression used to assess if distance and spatial scale affected the observed external transferability between the six study areas.

Formula: External transferability ~ distance + scale

Coefficients:

	Estimate	Std.error	t-value	P
(Intercept)	0.06	0.06	1.11	0.27
Distance	-0.00	0.00	-2.90	0.00
Spatial scale	0.21	0.05	4.48	0.00

Residual standard error: 0.6739 on 793 degrees of freedom
Multiple R-squared: 0.03473, Adjusted R-squared: 0.0323
F-statistic: 14.27 on 2 and 793 DF, p-value: 8.181e-07.

Appendix J2) Parameter estimates for the linear regression used to assess how the type of transferability (external/internal) and spatial scale affected the observed transferability.

Formula: Transferability ~ type * scale

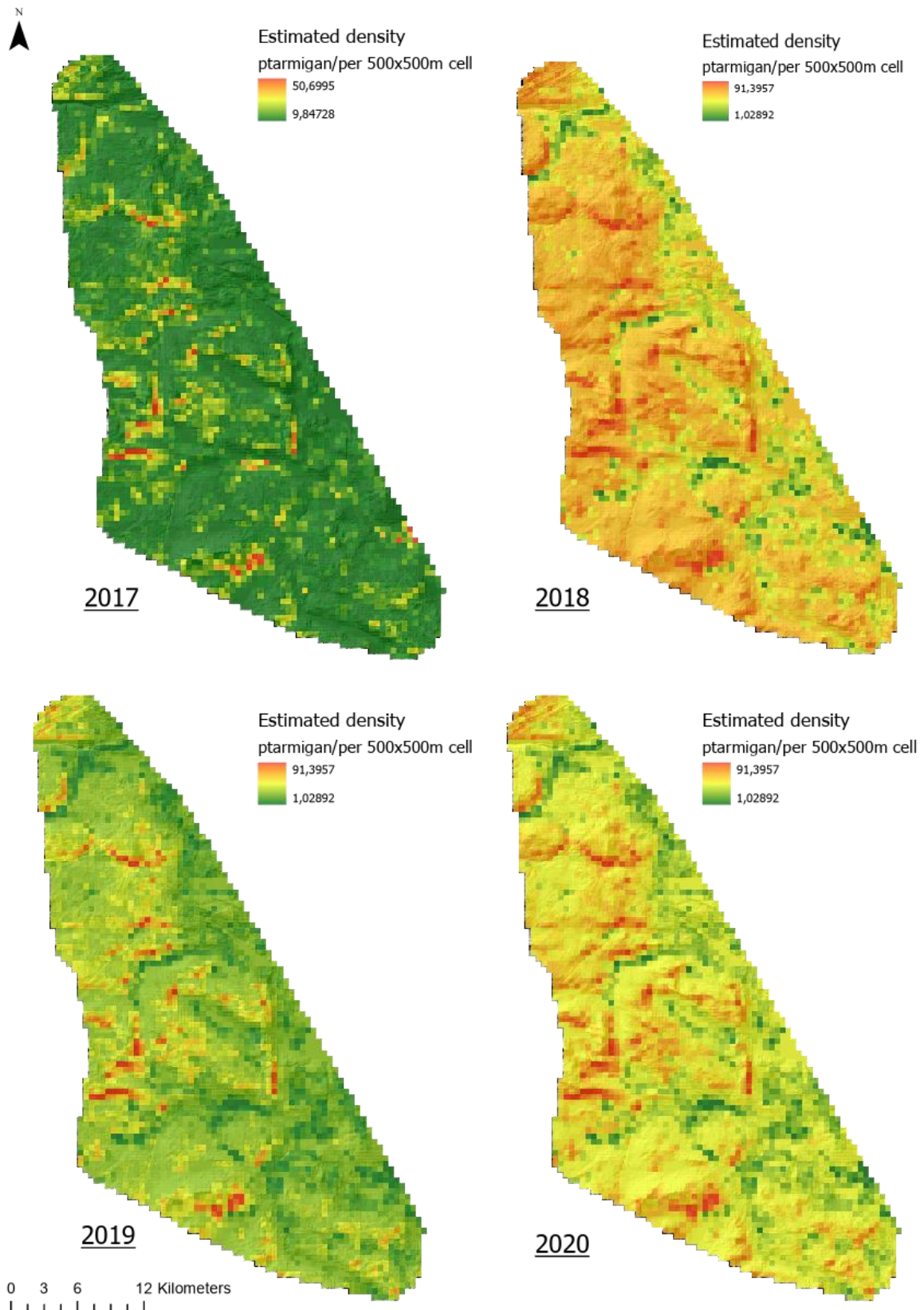
Coefficients:

	Estimate	Std.error	t-value	P
(Intercept)	-0.07	0.03	-2.00	0.05
Type: Internal	0.73	0.09	8.31	0.00
Scale: LS	0.21	0.05	4.61	0.00
TypeInternal: scaleLS	-0.34	0.12	-2.73	0.01

Residual standard error: 0.656 on 920 degrees of freedom
Multiple R-squared: 0.1012, Adjusted R-squared: 0.09831
F-statistic: 34.54 on 3 and 920 DF, p-value: < 2.2e-16

Appendix K

Appendix K1: Raster maps presenting estimates of the number of willow ptarmigan in 500 x 500m cells in study area 5 in the years 2017, 2018, 2019, and 2020. Maps are derived with local data, using a hierarchical distance sampling model with environmental covariates from a home range scale.



Appendix L

Appendix L1: Raster maps presenting estimates of the number of willow ptarmigan in 500 x 500m cells in study area 1 in the years 2017, 2018, 2019, and 2020. Maps are derived with local data, using a hierarchical distance sampling model with environmental covariates from a landscape scale.

